YC-154 SKYMASTER II

2006-2007 AIAA Undergraduate Team Aircraft Design Competition

VOLTAN
APPLIED AEROSPACE

VIRGINIA POLYTECHNIC INSTITUTE & STATE UNIVERSITY
DEPARTMENT OF AEROSPACE & OCEAN ENGINEERING

William S. Harrell
Team Leader / Mass Properties
AIAA 281818

John B. Shannon III
Aerodynamics
AIAA 247037

Ryan C. Koubek
Conceptual Design / Landing Gear
AIAA 249464

Michael G. Lunsford
Mission Performance
AIAA 235171

Paul E. Koerner
Stability & Control
AIAA 267566

Cameron A. Snider
Propulsion / Hight Lift / Cost
AIAA 274104

Patrick M. Maloy
Structures
AIAA 222319

Saleh M. Kausar
Systems / CAD
AIAA 217253

Dr. William H. Mason
Aircraft Design Professor
AIAA 11141

EXECUTIVE SUMMARY

The United States military is continuing to reduce its fighting force size. The future for the United States military is a highly trained, highly mobile force which makes use of the most advanced technologies available. With the United States Army moving in this direction, a modern air lifter must be provided to move these new highly mobile vehicles to where they will be of most use. This air lifter must be able to takeoff and land on the short and unimproved runway surfaces that are prevalent in the areas of modern conflict. This air lifter must also integrate seamlessly with today's commercial traffic in the Air Traffic Management (ATM) environment. The YC-154 Skymaster II provides an innovative solution to the problem of austere condition, inter-theater transport. By using proven technologies and innovative design integration, Zoltan Aerospace delivers a product that meets or exceeds all requirements set out in the AIAA request.

The YC-154 Skymaster II was designed to minimize drag incurred in the cruise portion of its mission. Landing gear pods were eliminated and the aircraft was carefully designed to eliminate as much upsweep as possible from the rear of the aircraft. A weight-saving strut-braced design was incorporated to create a light and efficient aircraft running two Pratt & Whitney F117 engines. The YC-154 Skymaster II is able to cruise at Mach 0.8 and complete either its combat mission or ferry mission on a single tank of gas.

To allow for short takeoff and landings an externally blown flap high lift system was incorporated into the design to allow as much lift as possible during the takeoff and landing segments of the mission. The YC-154 is able to takeoff in less than 2500 feet of runway.

The landing requirement forced the design to have enough control authority to allow a safe and short landing. The YC-154 can land and come to a full stop in 2100 feet; well within the

AIAA requirement of 2500 feet. The landing gear and thrust reversing systems were designed to facilitate landings on the short, unimproved surfaces outlined in the RFP.

The YC-154 Skymaster II will continue the venerable legacy of the Air Mobility command by providing immediate support anywhere at any time.

Requirement	RFP	Skymaster II	Reference
Cruise	Mach 0.8	Mach 0.82	Section 4.1
Service Ceiling	30,000 ft	40,000 ft	Section 3.5
Combat Mission			
Takeoff BFL	2500 ft	2380 ft	Section 3.3
Landing distance with a 5 knot tailwind component	3000 ft	2080 ft	Section 3.4
Capable of 25 knot crosswind landing	YES	YES	Section 7.6
Landing Surface CBR 4-6	YES	YES	Section 9.1
Ferry Mission			
Takeoff BFL	2500 ft	2230 ft	Section 3.3
Range	3200 nm	3414 nm	Section 3.2
Land	2500 ft	1560 ft	Section 3.4

I. TABLE OF CONTENTS

II. TABLE OF FIGURES

III. TABLE OF TABLES

IV. NOMENCLATURE

C_L	Lift coefficient
C_D	Drag coefficient
C_{D0}	Parasite drag coefficient
C_M	Pitching moment coefficient
C_T	Thrust coefficient
δe	Elevator deflection
δr	Rudder deflection
δa	Aileron deflection
δf	Flap deflection
δs	Slat deflection
α	Angle-of-attack
β	Sideslip angle
q	Dynamic pressure
ρ	Air density
σ	Density ratio
t/c	Thickness ratio
Λ	Wing sweep angle
M_{cr}	Critical Mach number
V_{stall}	Stall speed
T	Thrust
S	Wing area
BFL	Balance field length
OEI	One engine inoperative
γ	Landing approach angle
V_f	Flare velocity
c_w	Wing chord
t/c	Thickness to chord ratio
W/S	Wing loading
T/W	Thrust to weight ratio
AR	Aspect Ratio
L/D	Lift to drag ratio
MAC	Mean aerodynamic chord
TOGW	Takeoff gross weight
BPR	Bypass ratio
SFC	Specific fuel consumption
ECS	Environmental control system
OBIGGS	Onboard inert gas generating system
STOL	Short takeoff and landing
CBR	California bearing ratio
RDTE	Research, development, test and evaluation
RFP	Request for proposal

V. FOLDOUTS

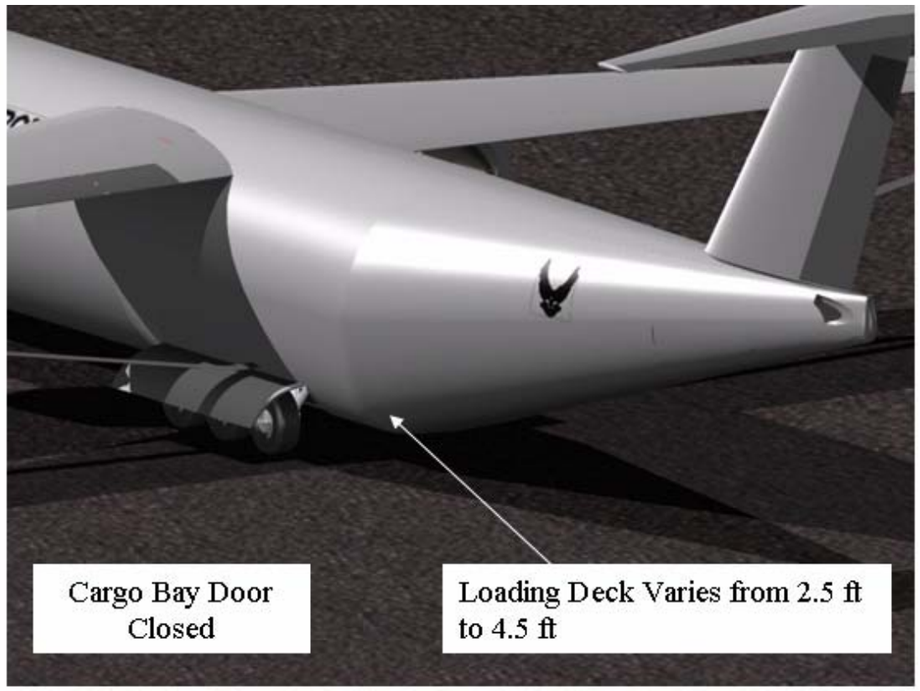

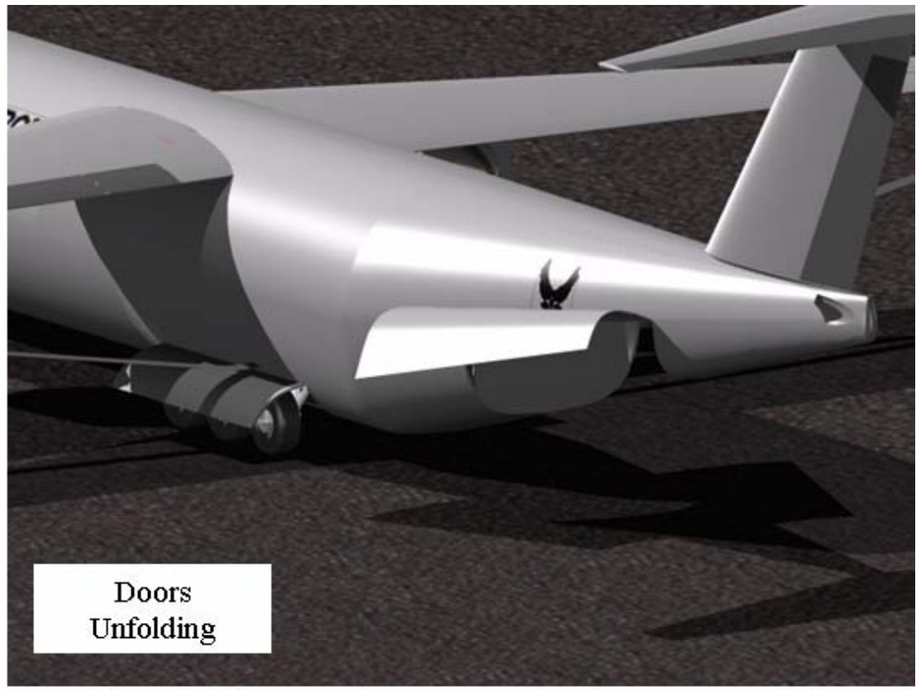

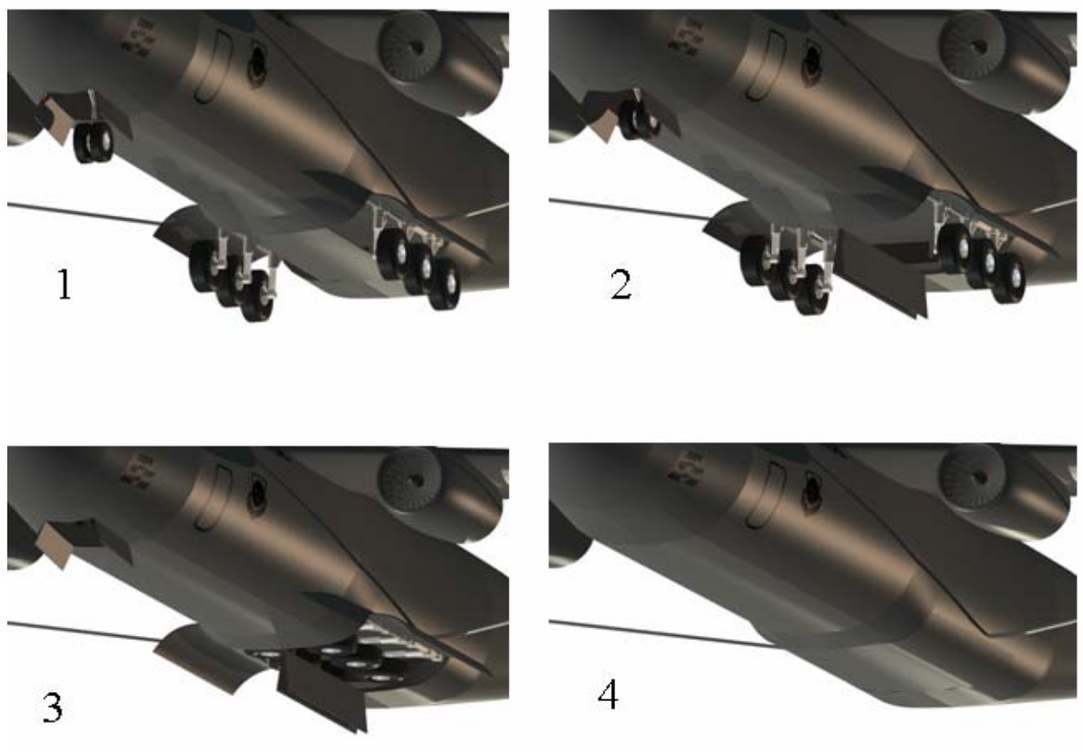

Landing Gear Sequence

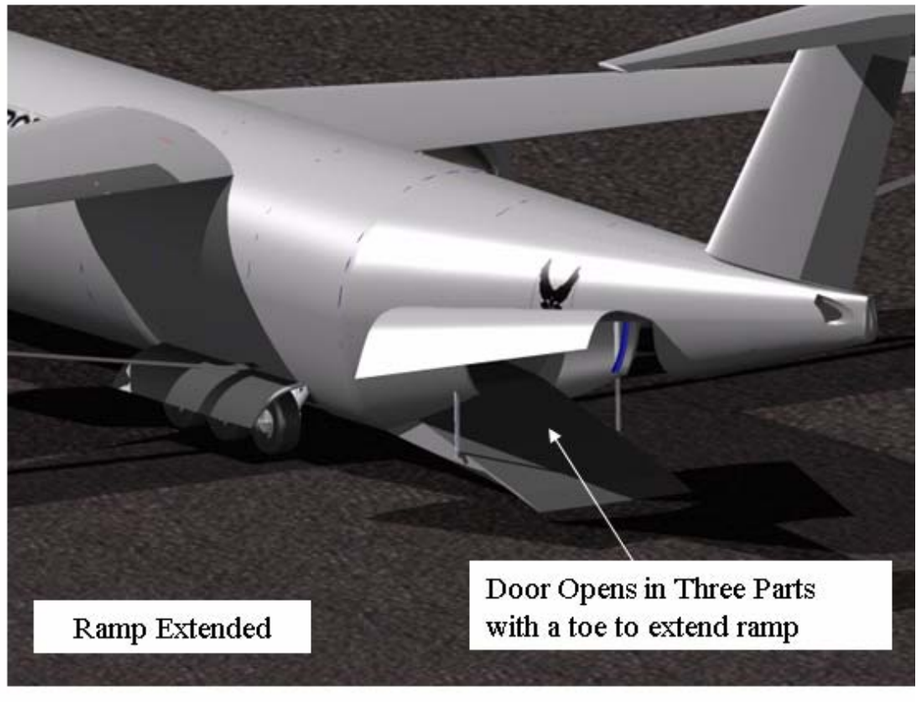

Figure V.1: Cargo Bay Door and Landing Gear System

Geometry	
Wing Area	2000 ft^2
Aspect Ratio	10
Wing Loading	91 lbs/ft^2
Leading Edge Sweep	15°
Trailing Edge Sweep	0°
Vertical Tail Area	352 ft^2
Vertical Tail Sweep	38°
Horizontal Tail Area	259 ft^2
Horizontal Tail Sweep	20°

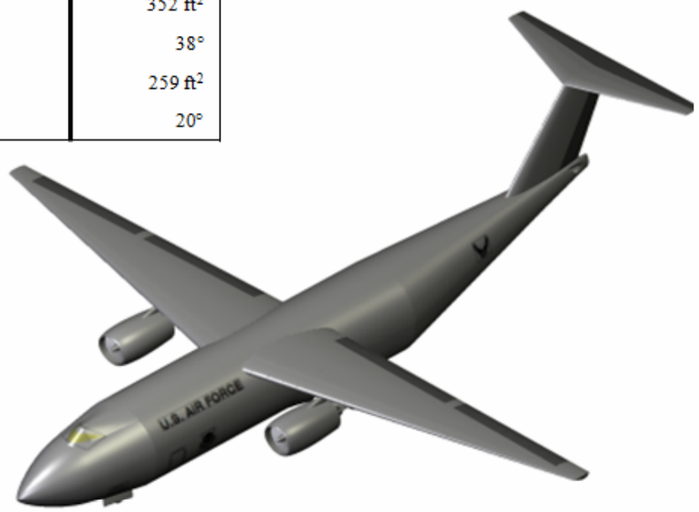

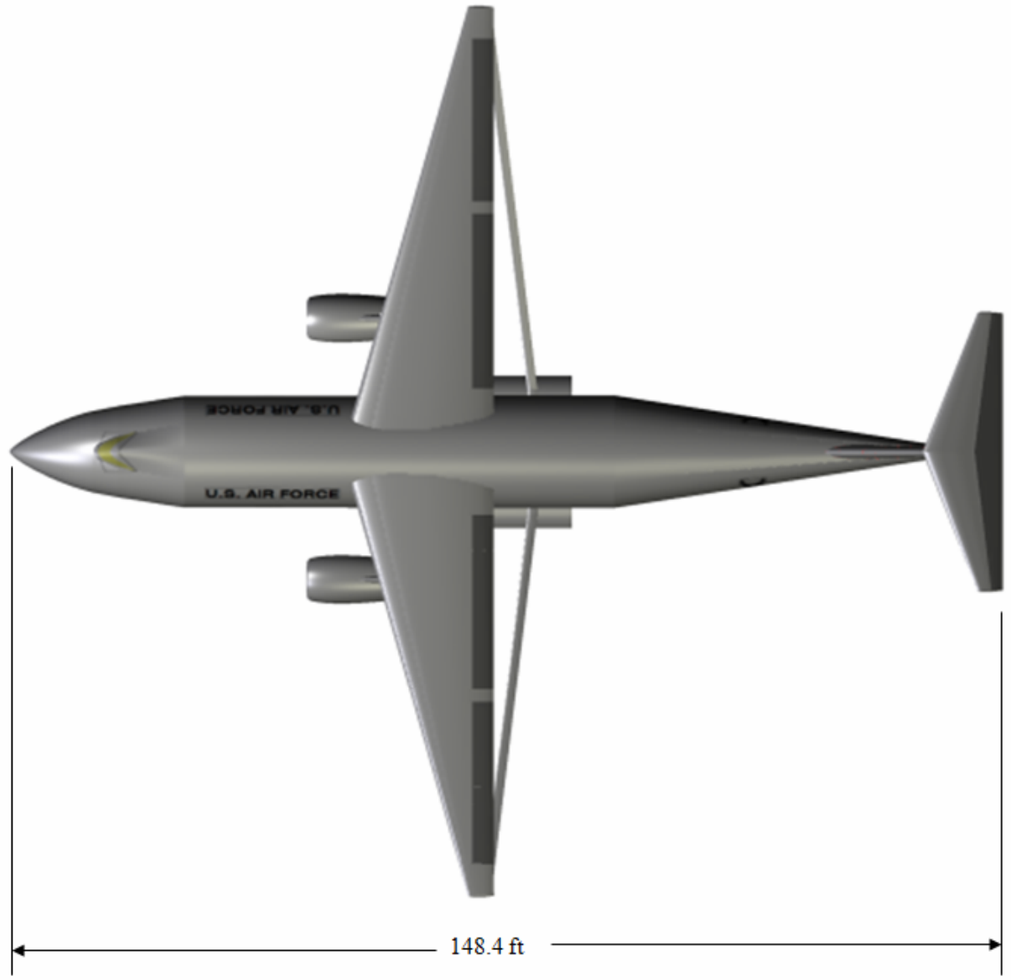

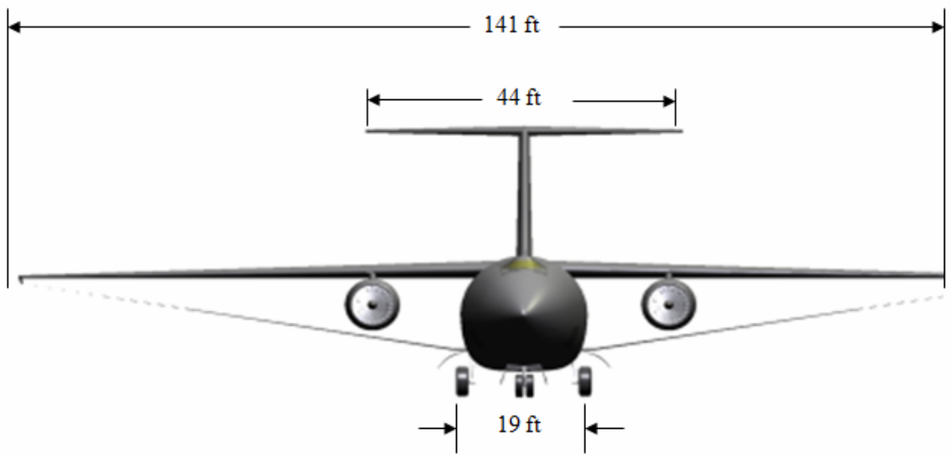

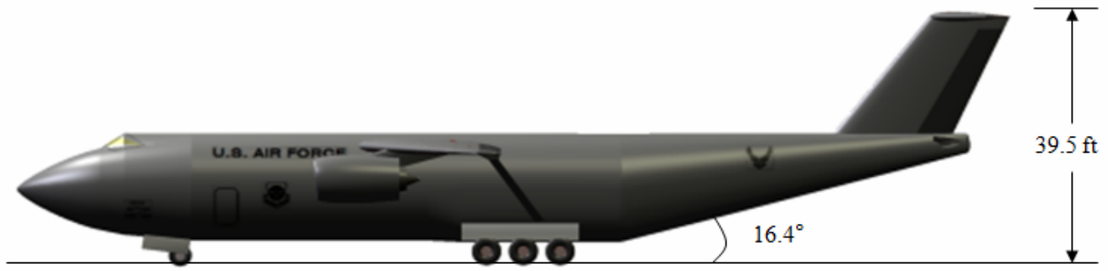

Figure V.2: Dimensioned Three View Layout

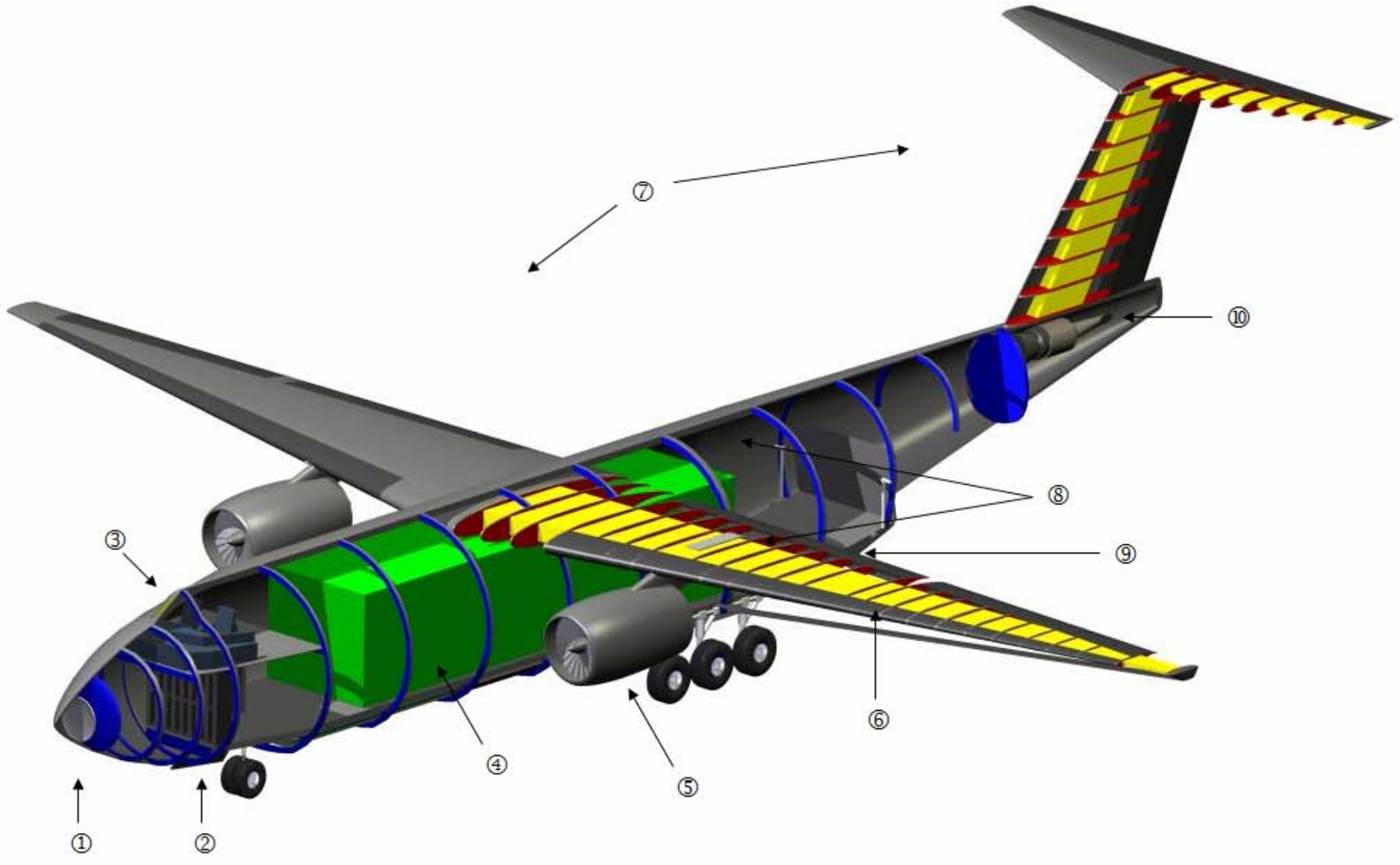

① • 22 in. Tilt Angle Weather, Traffic & Terrain Radar
• Missile Warning / Infrared Search & Track

② • E/E Racks
• LRU Cooling

③ • Integrated Avionics Suite

④ • FDAV 50,000 lbs.
• Support Equipment 10,000 lbs.

⑤ • Pratt & Whitney F117-PW-100
• 90 kVA IDG 115/200 V 400 Hz AC

⑥ • Integral Wing & Center Fuel Tanks
• OBIGGS
• JP-8 10.500 gal.

⑦ • Electro-hydrostatic & Electromechanical Actuators

⑧ • Automatic Fire Detection & Suppression

⑨ • Drybay Auxiliary Fuel Cells

⑩ • APU 90kVA Generator
• Countermeasure Dispensing System

Figure V.3: Internal Layout

Figure V.4: Structural and Materials Layout

1. Overview of Proposal

1.1 Introduction

> Air Mobility Command's mission is to provide rapid, global mobility and sustainment for America's armed forces. The command also plays a crucial role in providing humanitarian support at home and around the world. The men and women of AMC - active duty, Air National Guard, Air Force Reserve and civilians - provide airlift and aerial refueling for all of America's armed forces. Many special duty and operational support aircraft and stateside aeromedical evacuation missions are also assigned to AMC. U.S. forces must be able to provide a rapid, tailored response with a capability to intervene against a well-equipped foe, hit hard and terminate quickly. Rapid global mobility lies at the heart of U.S. strategy in this environment - without the capability to project forces, there is no conventional deterrent. As U.S. forces stationed overseas continue to decline, global interests remain, making the unique capabilities only AMC can provide even more in demand.
>
> *– Air Mobility Command Mission Statement*

The United States Air Force Air Mobility Command (AMC) has been gallantly serving the United States since the early years of aviation. The men and women of the AMC have flown the “Hump” in Burma, provided relief to the oppressed people of Berlin during the Berlin Airlift, relieved beleaguered Marines and Army personnel at the Chosin Reservoir, evacuated POW’s from the infamous Hanoi Hilton during the Vietnam War, and continued to provide extraordinary service throughout the recent conflicts in Iraq and Afghanistan.

Throughout these conflicts, the aircraft that the AMC has utilized have changed significantly. From the venerable C-47 Skytrain, C-46 Commando, and the C-54 Skymaster of the early years, to the C-17 Globemaster III, C-5 Galaxy, and the C-130 Hercules, the names

have changed but the mission has stayed constant; providing airlift service for the men and women of all services. To continue the level of excellence that the AMC has provided, it is imperative that improvements in capabilities continue to be made. This can only be done through tireless work and dedication.

The United States military is continuing to emphasize the reduction in force size. The future is a small, highly trained force, which makes use of the most advanced technologies available in order to protect our way of life. The days of massive main battle tanks rolling across the plains of Europe are over, in its stead, the more fluid and changing modern battlefield is coming to fruition. With the United States Army moving away from their large and heavy vehicles, a modern air lifter must be provided to move these new vehicles into and out of the battlefield. This air lifter must be able to takeoff and land on the short and unimproved runway surfaces that are prevalent in the areas of modern conflict. Current aircraft leaves the AMC with a gap in its ability to move into and out of these areas. C-130 Hercules has the capability to land and takeoff in these areas, but with a limited payload that won't allow for Future Combat Systems vehicles to be moved with any great efficiency and the C-17 which is too heavy and too powerful to operate out of these forward locations. This gap must be filled in order for the AMC to continue to provide the level of support that it currently achieves.

Figure 1.1: C-54 Skymaster (circa 1946)

The answer to this need is the C-154 Skymaster II. Named for the venerable C-54 Skymaster, which preformed gallantly in World War II and the Berlin Airlift, this new aircraft will seek to continue in the extraordinary tradition of service set forth by its predecessor. This new aircraft will be able to takeoff and land on the short, unimproved airfields of the forward operating locations in which today's soldiers, airmen, and marines find themselves everyday; allowing them to take the fight to the enemy. It will also be able to perform much like today's modern airliners, allowing for savings in time and money during operations.

1.2 Requirements Presented in Request for Proposal

The AIAA Design Competition Request for Proposal (RFP) calls for an air lifter that is designed to support the U.S. Army's need for future tactical warfare mobility. This requires an aircraft that can operate in an inter-theater tactical environment and out of small and unimproved airfields. The design payload is the U.S. Army Future Deployable Armored Vehicle (FDAV). Moving this vehicle into and out of areas of opportunity will allow the soldiers who operate it to take the fight to the enemy at a moments notice and will also reduce the necessity of dedicated airfields for Air Mobility operations. The ability to operate out of combat operations areas will

require a versatile vehicle with short takeoff and landing (STOL) capabilities and will allow the U.S. Air Force the flexibility to keep up with today's rapidly changing battlefield situations. The aircraft will also be required to integrate into the air-space infrastructures of the United States and abroad. To meet this requirement the aircraft will need to possess commercial airliner speeds and cruise altitudes and be self-deployable as well.

Specifically the aircraft must be capable of carrying the large and outsized payloads such as the FDAV, which weighs 25 tons. The aircraft also must carry the 5 tons of support equipment that will allow the FDAV to operate once it hits the ground. The cargo bay dimensions must be at minimum 560" long by 128" wide by 114" high. These dimensions include a 12" escape path around the vehicle.

The aircraft must have STOL capabilities to allow it to accomplish its mission. Specifically the aircraft must have a critical field length of 2000-3000 feet. The runway surface is unimproved with a California Bearing Ratio (CBR) of 4-6. It also will require all weather/nighttime capability to allow it to operate in any type of conditions. With the Air Force operating during all hours of the day and night, and with the possibility of having to takeoff and land in a hostile area, noise mitigation will be an issue that will need to be resolved. Not only will it be important to the civilians living in the vicinity of these Air Force bases, but it will also be critical to the air lifter's survivability.

Along with the air lifters short field requirements, it also must be capable of cruising at an altitude of 30,000 feet and obtain a cruise Mach number of 0.8. Its ferry range will be 3000 nm but it may be refueled in flight.

The aircraft must also integrate well into the "network-centric battlefield". The "network-centric battle space" is a relatively new concept. It links all the forces in a theater of combat

together to allow information sharing. This increases situational awareness, shortens the "kill-chain" and allows joint forces to operate seamlessly. Being able to integrated into this system will be incredibly important in future combat scenarios. Given the current trend of non-linear, urban warfare type conflicts, flexibility and situational awareness will be a key to victory.

1.3 Mission Identification and Analysis

There are two key missions that the aircraft will have to fly. The primary mission is a combat mission that involves flying the aircraft to an austere and possibly hostile landing site, dropping its payload, and returning to base. The secondary mission is a long haul ferry flight with minimal payload. A crew of three which includes a pilot, a co-pilot, and a loadmaster will fly both missions. Both missions are important to the success of the aircraft; however early on it was determined that the combat mission will be the driver of the design.

1.3.1 Combat Mission

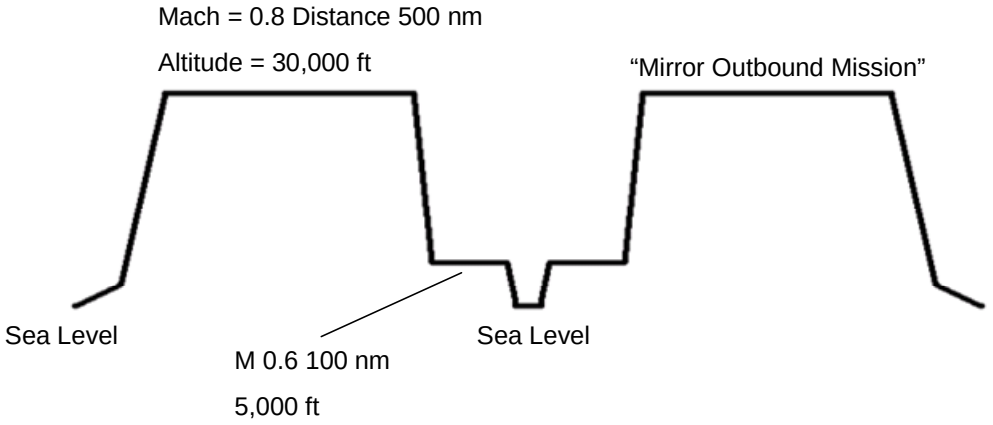

Figure 1.2: Combat Mission Visualization

The combat mission begins with the aircraft start-up, warm-up, and taxiing at idle power for 8 minutes before takeoff. The takeoff portion is considered to use two minutes worth of fuel at maximum power. The next segment is a climb/cruise to best cruise altitude. Following that is a

high-speed cruise of 500 nautical miles at a Mach number of 0.8. The aircraft will then descend to 1000 feet for 100 nautical miles at a Mach number of 0.6. The aircraft will then descend to land. Due to the opportunistic nature of where the runway is located the aircraft must be able to land in a 25-knot crosswind with a 5-knot tailwind component. The aircraft will then takeoff under combat rules, meaning there is no assumed engine failure and there is a 50-foot obstacle over which the aircraft must climb. The egress portion of the mission will mirror the ingress portion. It should be noted that the aircraft is loaded with the full 30-ton payload for the combat mission.

1.3.2 FERRY MISSION

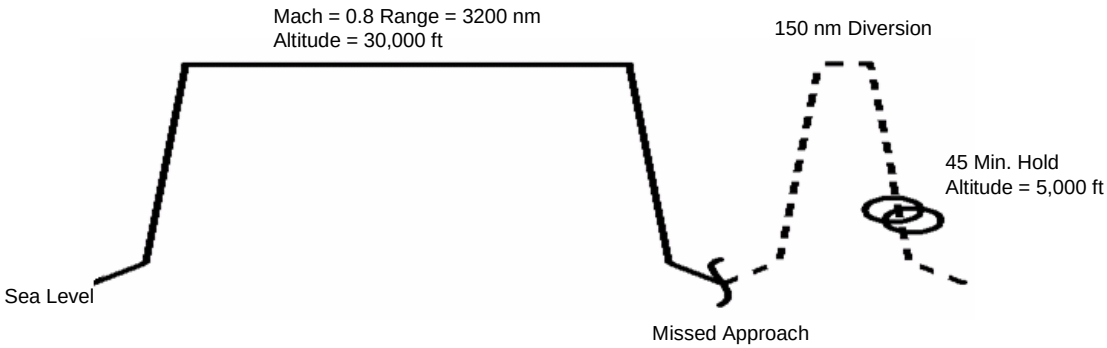

Figure 1.3: Ferry Mission Visualization

The ferry mission begins in a similar fashion as the combat mission; however the aircraft will be only loaded with 10 tons of bulk cargo. This cargo will have a density of 20 lb/ft^3. The aircraft will start-up, warm-up, and taxi for 8 minutes then takeoff. It will then climb to best cruise altitude and cruise at a Mach number of 0.8 for 3200 nautical miles. Mid-air refueling is permitted during this segment and the number rendezvous and quantity of fuel brought on board will have to be noted. The aircraft will descend and land then taxi and park using idle power for 10 minutes. Reserve fuel must be factored in for a missed approach, a 45 minute hold at 5,000 feet and a 150 nautical mile diversion.

1.4 Identification of Mission Drivers and Analysis

To begin the conceptual design process, it was important to first identify the areas of the mission that would be the basis for the aircraft's success or failure. Three areas of concern were identified: cruise, takeoff, and landing. Each of these areas had its own unique requirements in order for RFP requirements to be met. Designing the aircraft to mitigate these contrasting requirements became the overriding objective.

1.4.1 Cruise Performance

The most challenging requirement set out in the RFP was not the most obvious at first. Cruise drag is a large area of concern for this design. After some initial research was done on comparator aircraft it was found that few, if any, could achieve the cruise performance that was within the RFP specifications. Landing gear pods were removed in favor of better integration of landing gear, wing loading was set to 91 lbs/ft^2, and a strut-braced wing was designed to allow for a longer span and thinner airfoil cross section. This eliminated the need for four engines and allows the YC-154 to cruise at 0.8 Mach at 30,000 feet.

1.4.2 Takeoff

The takeoff segment of the flight was the major concern during the initial stages of conceptual design. It was understood that a low wing loading is generally a positive attribute of a STOL aircraft. This lower wing loading came into direct interference with the cruise performance requirement. To mitigate this, an externally blown flap system was developed to allow for a C_{Lmax} of 4.2 and allows the YC-154 to takeoff in less than 2500 feet of runway.

1.4.3 LANDING

The landing requirement was not as straightforward as it might first appear. First there is the distance requirement that must be analyzed with a 5 knot tail wind. The YC-154 can land and come to a full stop in 2100; well within the AIAA requirement of 2500 feet. The surface impact requirement drove the size and complexity of the landing gear system. A California Bearing Ratio 4-6 type surface is extremely soft and is equivalent to a packed sand and clay surface and it is imperative to be able to handle these types of surfaces. The YC-154's main landing gear consist of six 53 inch tall and 18 inch wide tires that are only inflated to 50 pounds per square inch. This allows the Skymaster II to meet the requirement for landing surface.

2 CONCEPTUAL DESIGN

2.1 INTRODUCTION

Initially three preliminary concepts were developed as to allow for a broad study to be conducted of designs that could possibly meet the mission requirement. In the end of the process not one of these designs was picked explicitly, however aspects of each design were integrated to create a better suited aircraft. The three designs are as follows: a high mounted, strut-braced wing aircraft with a conventional tail, a high mounted wing with a boom tail aircraft, and an upper surface blowing concept with a T-tail. The fuselage dimensions of each aircraft were similar, the fuselage length being 110 feet with a diameter of 16 feet. Each concept was designed with a different aspect ratio wing to allow for a study to be done on the effect aspect ratio has on takeoff gross weight.

Figure 2.1: Composite of each preliminary concept

2.2 CONCEPT ONE

Figure 2.2: Concept One: High Mounted Strut-braced Wing

Concept one is a conventional looking aircraft. The major design point was the addition of a strut-braced wing. The wing itself was designed to have an aspect ratio of 6, however, after some research it was found that the major advantage of having a strut-braced wing configuration is the ability to extend the wingspan and in turn raise the aspect ratio. This was not identified early enough in the design process and was rectified when picking a preferred concept. This configuration was analyzed and the design space for this aircraft was identified. The TOGW of this aircraft was determined to be 240,000 pounds and its C_{Lmax} was set at 4.0. The TOGW estimation is high because the aspect ratio of the wing is not optimized to take advantage of the strut as previously mentioned.

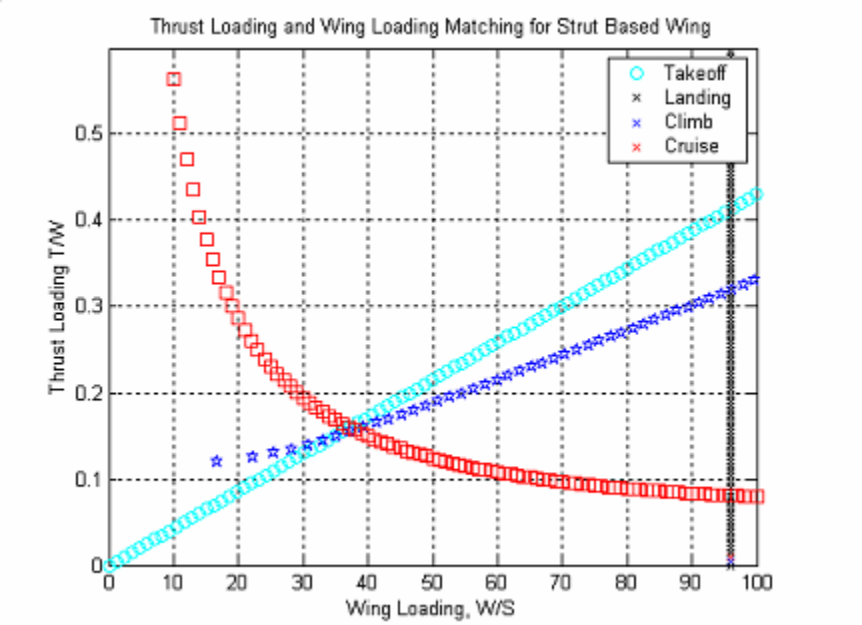

Figure 2.3: T/W vs. Wing Loading Diagram for Concept 1

2.3 CONCEPT TWO

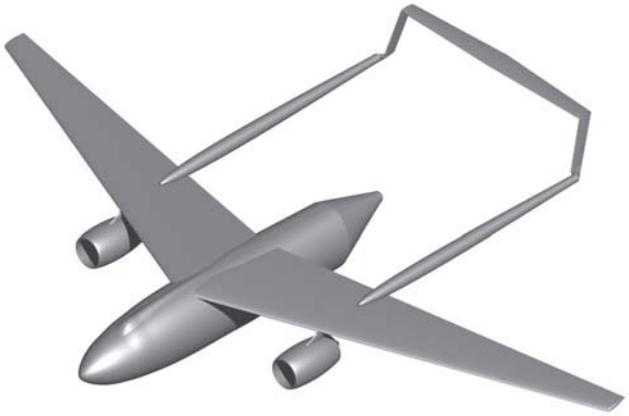

Figure 2.4: Concept Two: High Mounted Wing, Boom Tail

Concept two was designed to look similar to a C-119 Flying Boxcar aircraft. The aircraft features a boom tail configuration with a wing aspect ratio of 10. This high aspect ratio, which without a strut would result in a heavy wing, led to a TOGW of 219,000 pounds. Because no strut was incorporated into this design it is unfeasible that this TOGW would be able to be achieved. The amount of structure the wing would need would offset any weight savings that a high aspect ratio will allow. This concept also had significant problems with upsweep angle

mitigation due to concerns about loading the design payload. Steps were taken to mitigate this effect. However, cruise drag was significantly increased. The C_{Lmax} of this design was also considered to be low, at 3.4, leading to unrealistic requirements for wing loading and thrust to weight.

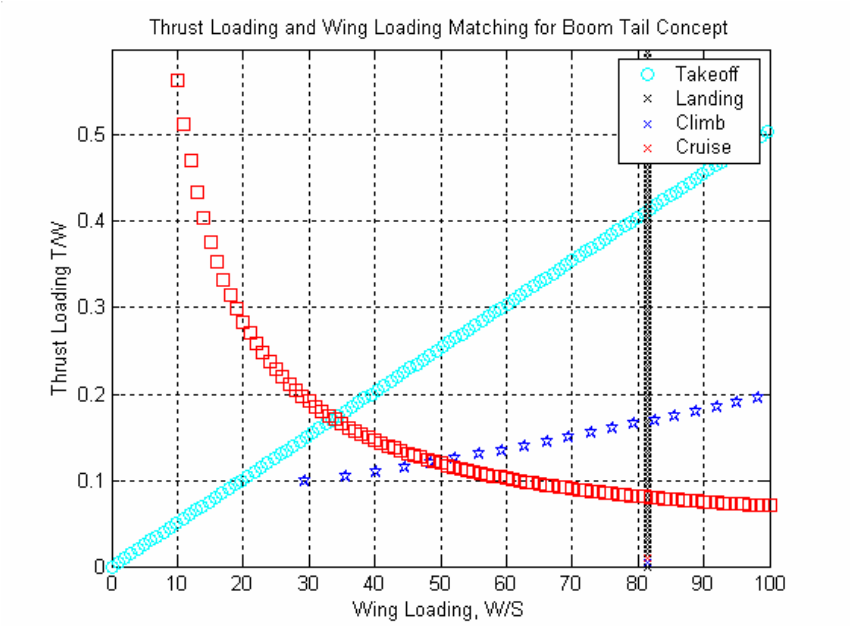

Figure 2.5: Concept 2 Design Space

2.4 CONCEPT THREE

Figure 2.6: Concept Three: Upper Surface Blowing, T-Tail

Concept Three was developed as an upper surface blowing configuration that led to a high initial C_{Lmax} of 5. The wing aspect ratio was set at 8 leading to a TOGW of 227,000 pounds.

The effect of increasing the maximum lift coefficient was that the wing loadings could be made higher. These higher wing loadings allow for more efficiency in cruise and will alleviate issues with meeting the stringent cruise requirement. Placing the engines on top of the wing has many adverse effects, one being a significant pitch down moment that is generated when the engine is moved further off the center of gravity axis. This effect is important to consider when dealing with a STOL aircraft that will need as much horizontal stabilizer authority as possible.

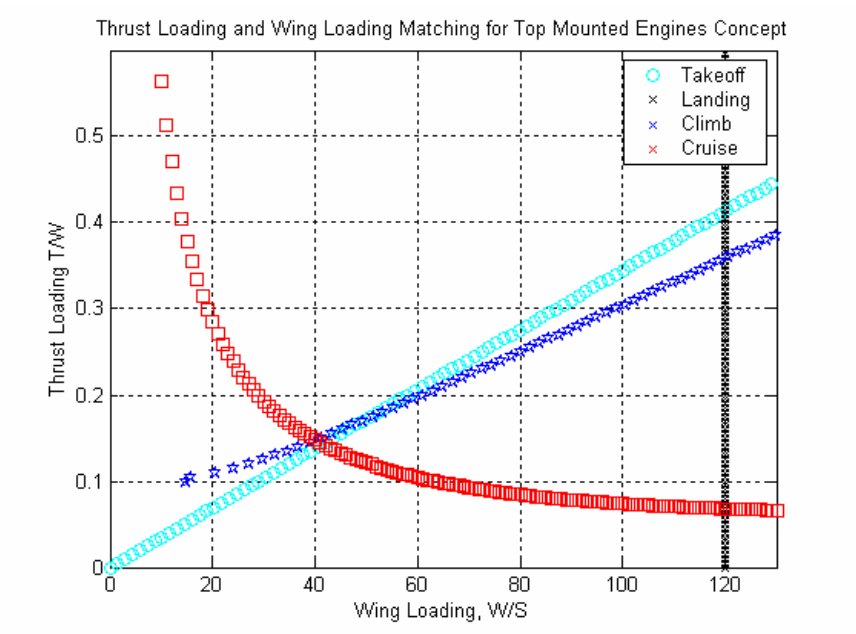

Figure 2.7: Concept 3 Design Space

2.5 PREFERRED CONCEPT DOWNSELECT

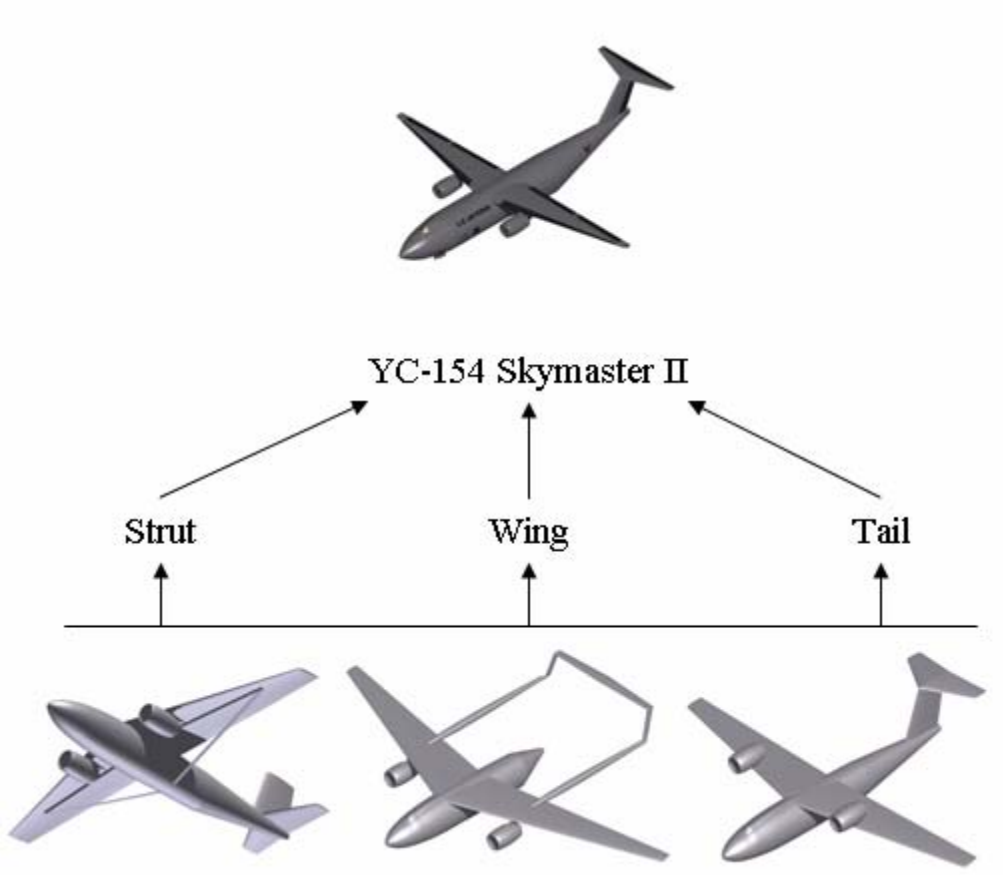

Figure 2.8: Concept Down Select

After weighing all of the feasible options that were identified in the conceptual design phase a conglomeration of all three designs was chosen to take forward into preliminary design. The key dimensions aircraft would then be taken through much iteration to fully develop the aircraft that is being proposed. Table 2.1 shows what the key dimensions of the aircraft were at the beginning of the preliminary design and what they are currently being proposed. Significant changes were made throughout the process as problems arose and were dealt with. Several key areas should be noted.

One of the first major changes was the wing loading of the aircraft. After the aerodynamics was studied for drag at cruise conditions it was found that we underestimated the

impact that drag had on the size of the wing. The wing loadings therefore of our first three designs were extremely low due to the large wings we had envisioned on those aircraft. The wing planform was reduced to help meet the cruise requirements of 0.8 Mach. The next design iterations went from as high as 120 lbs/ft^2 to a more reasonable 91 lbs/ft^2.

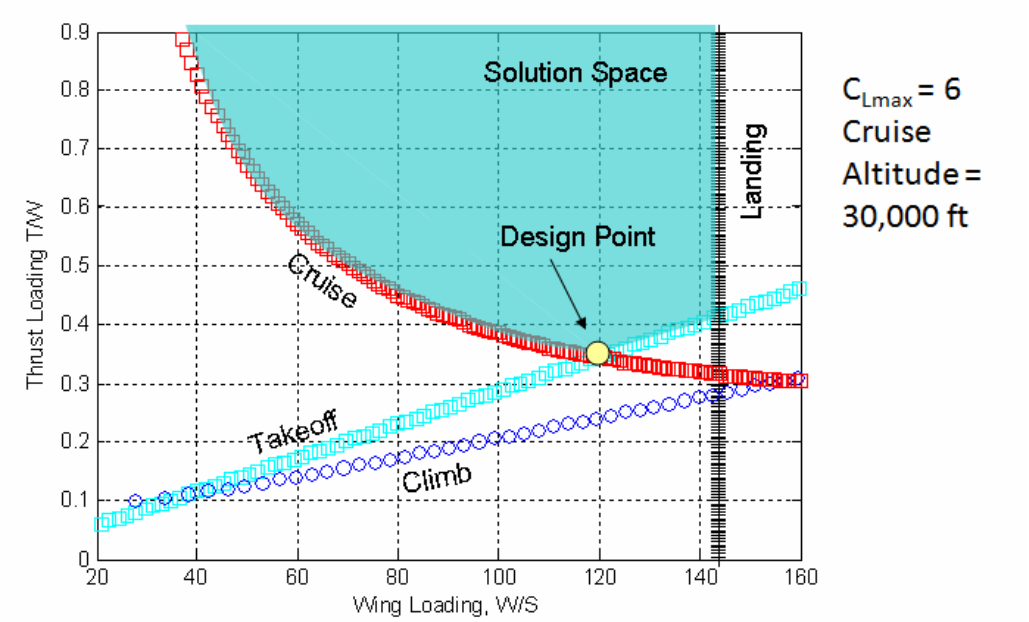

Figure 2.9: YC-154 Blk 0 Design Space

As Figure 2.9 shows, a new cruise design constraint was used which dramatically increased the required T/W and W/S of the aircraft due to the more detailed drag analysis. This aircraft was designated the YC-154 Blk 0 aircraft since it most matched our current design approach.

The high lift system also saw drastic changes during the initial conceptual designs. The initial weight estimates were extremely conservative putting the aircraft at 220,000 lbs. A more accurate weight method would later be developed, but in the meantime this required a large C_{Lmax} for the aircraft to meet its balanced field length requirement set out in the request for proposal. This required the use of a powered lift type system and the augmentor wing seemed to fit.

Due to difficulties integrating the augmentor wing with the propulsion system and after reworking the weights, it was determined that a much lower C_{Lmax} was sufficient to meet the balanced field length. The augmentor wing was then abandoned in favor of the simpler to integrate and industry accepted externally blown flap system.

As the drag and propulsion estimations became more refined the aircraft's takeoff gross weight became lower as drag decreased and methods of estimation became more refined, leaving an 182,000 lb aircraft.

Table 2.1: Preferred Concept Evolution

Key Dimensions	YC-154 Blk 0	YC-154 Blk 1
Weight	220,000 lbs	182,000 lbs
Wing Planform Area	1833 ft^2	2000 ft^2
Wing Span	138 ft	141.5 ft
Wing Sweep	15 degrees @ LE	15 degrees @ LE
Wing Aspect Ratio	10	10
Wing Loading	120 lbs/ft^2	91 lbs/ft^2
Thrust To Weight	0.35	0.42
C_{D0} / C_D @ Cruise	0.023 / .030	0.0236 / 0.0296
C_{Lmax}	6.5	4.0
Number of Engines	2	2
Type of Engines	Pratt and Whitney F117	Pratt and Whitney F117
High Lift System	Augmentor Wing	Externally Blown Flaps
Horizontal Tail Area	452 ft^2	352 ft^2
Vertical Tail Area	358 ft^2	259 ft^2

3 PERFORMANCE AND SIZING

3.1 PRELIMINARY SIZING

The combat mission was used in the preliminary sizing of the aircraft since it was determined to be the most demanding of the two missions. Not only must the aircraft takeoff with a balanced field length of 2,500 feet or less and carry a 60,000 payload 600 nm to a short runway, but it also must land in unfavorable winds and return to base after dropping the payload.

The initial mission segments are displayed in Figure 3.1. Their resulting weight fractions are tabulated in Table 3.1 and were found using methods from Raymer (Ref 2).

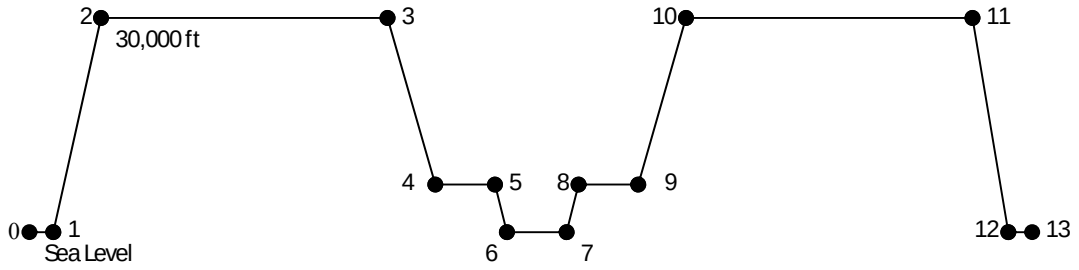

Figure 3.1 Initial Combat Mission Profile

Table 3.1: Mission Segments and Weight Fractions

Segment	Description	Weight Fraction
0-1	Warm-Up and Takeoff	0.980
1-2	Climb to 30,000 ft	0.979
2-3	Mach 0.8 Cruise 500 nm	0.941
3-4	Descend to 1000 ft	0.994
4-5	Mach 0.6 Cruise 100 nm	0.987
5-6	Descent for Landing	0.995
6-7	Land and Drop Payload	0.980
7-8	Climb to 1,000 ft	0.995
8-9	Mach 0.6 Cruise 100 nm	0.987
9-10	Climb to 30,000 ft	0.979
10-11	Mach 0.8 Cruise 500 nm	0.941
11-12	Descend for Landing	0.994
12-13	Land	0.994

The initial total mission fuel fraction was found to be 0.534 after adjusting for the payload removal between segments 6 and 7.

One of the first factors of the aircraft sizing investigation was the maximum lift-to-drag ratio $(L/D)_{max}$. *L/D* has a strong influence on the aircraft's takeoff gross weight (TOGW). A higher $(L/D)_{max}$ allows for a lighter weight airplane which is beneficial in almost all aspects of design. However, this requires a larger aspect ratio (*AR*). Constraints on the aspect ratio include wingspan and wing planform area. To reduce the weight of the aircraft an aspect ratio of 10 was

decided for the design which is higher than most military transports and gave us an $(L/D)_{max}$ of 15.85.

An initial takeoff gross weight of 220,000 pounds was found using a method developed by Nicolai (Ref 3) that made use of the weight fractions from Table 3.1 along with estimations of fixed equipment weight and an empirical weight formula. Fixed weight estimations included 600 pounds accounted for the aircraft crew, 60,000 pounds of payload to be dropped, and miscellaneous equipment of 10,000 pounds. Iterations were done until a weight solution was found where required weight equaled available weight. The fuel weight was calculated to be 45,116 pound from the analysis which accounts for 6% extra fuel as reserves.

The empty weight of the aircraft was further refined using statistical analysis of aircraft parts using Roskam (Ref 4). The initial weight estimates used in the Nicolai (Ref 3) method and were conservative and therefore on the heavy side. Further refinement of TOGW included better estimates of the aircraft systems weight as our design developed, takeoff balanced field length calculations, and thrust available in cruise. These refinements led to a resized aircraft weight of 185,000 lbs. Figure 3.2 shows the thrust to weight (T/W) vs. wing loading (W/S) for this aircraft. The yellow dot indicates where the design fell in relation to these parameters. Figure 3.2 assumed a 30,000 ft cruise altitude and a C_{Lmax} of 5.0.

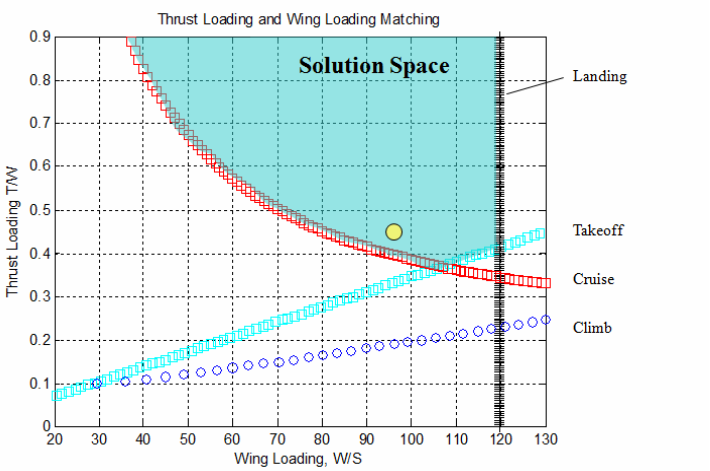

Figure 3.2 Thrust vs. Weight and Wing Loading for 185,000 lb Solution

Again further refinements to the aircraft led to another weight iteration. Changes in the mission profile to conserve fuel and a push for a smaller C_{Lmax} to help with the high lift system, along with stability issues moved the design to the final TOGW of 182,000 lb.

A trade study was developed to ensure the lowest weight solution was used. Below in Figure 3.3 shows a carpet plot of aircraft weight vs. wing loading and thrust to weight for the austere transport in the combat mission configuration.

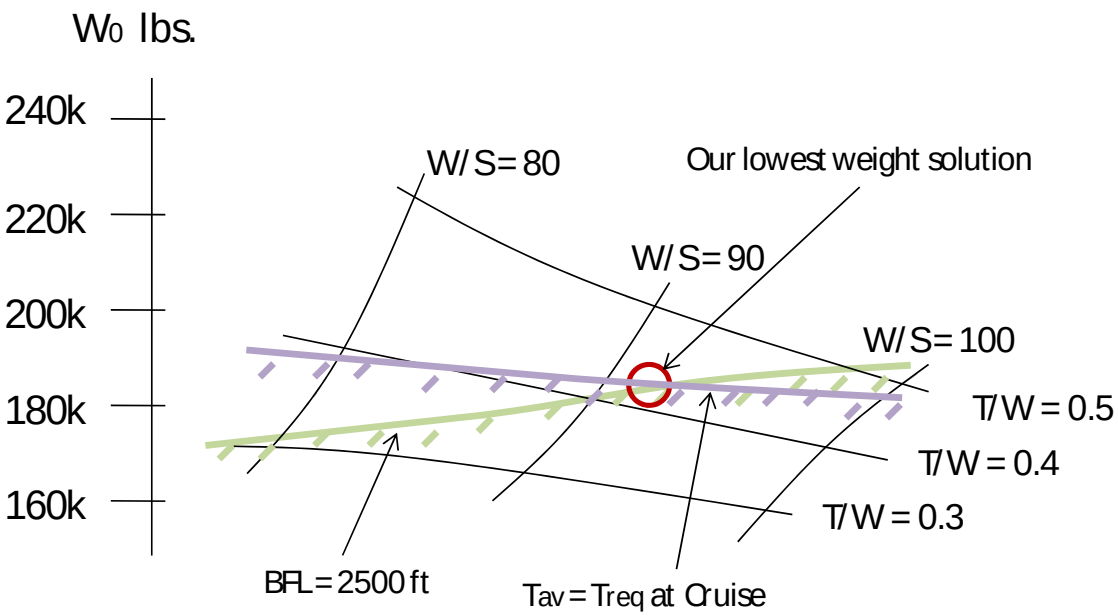

Figure 3.3 Aircraft Weight vs. T/W and W/S Carpet Plot

The lowest weight solution was confirmed to be near 182,000 pounds where the aircraft is still able to meet all of its requirements. It was found that the most critical performance requirements of the aircraft were the takeoff balanced field length and the thrust to sufficiently overcome the drag in cruise. The final C_{Lmax} used was 4.0, a product of externally blown flaps, which was confirmed by test data and discussed in the high lift section.

The final T/W vs. W/S diagram is shown below in Figure 3.4. The current design point coincides with the saddle point on the graph where the lowest T/W occurs at a point between the takeoff and cruise requirements of the design. The aircraft has a thrust to weight of 0.42 and a wing loading of 91at the TOGW, sea level static thrust condition.

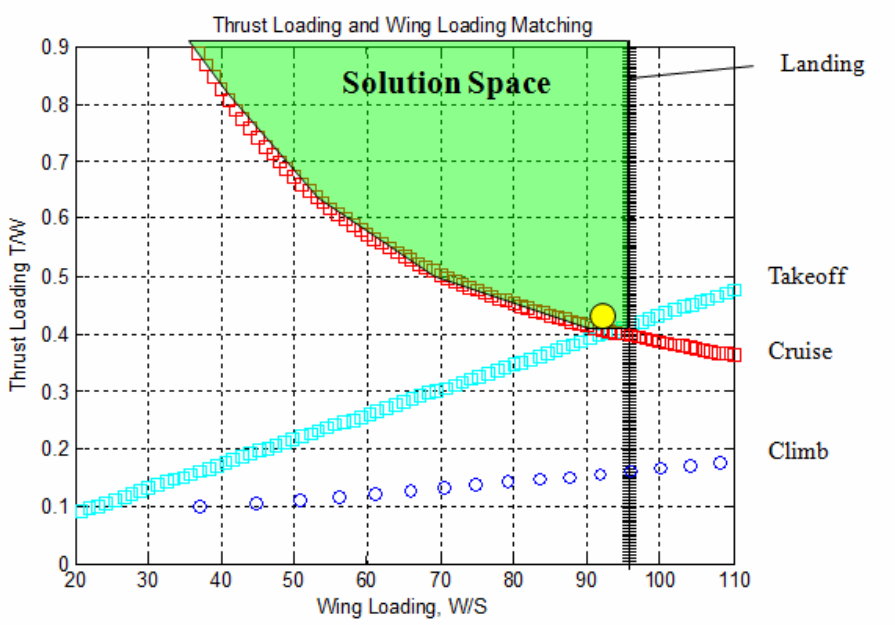

Figure 3.4 Skymaster II T/W vs. W/S Solution

Figure 3.4 differs from 3.2 in that it is shifted to the left. This shift reflects the lower C_{Lmax} value used calculating landing and takeoff distances. There are many advantages in lowering the aircraft's dependence on C_{Lmax} due to the complexity of high lift systems. Engine out or other mechanical failures could impact the aircraft's ability to maintain high C_{Lmax} values. Aircraft longitudinal stability also is enhanced by lessening the need for a higher C_{Lmax}.

3.2 MISSION PERFORMANCE

The entire combat and ferry mission performance was calculated based on the engine deck, expected drag, and mission profile. A Matlab program developed by Chris Cotting (Ref 24) was used to find performance characteristics such as time, altitude, range, fuel, fuel flow, and speed. The required aircraft fuel was found from iterating fuel weights and running the mission profile program. Table 3.2 illustrates the combat mission profile with the aircraft performance characteristics at each segment displayed.

Table 3.2 Combat Mission Profile

Inter-Theater Tactical Transport with Austere STOL Capability COMBAT MISSION PROFILE

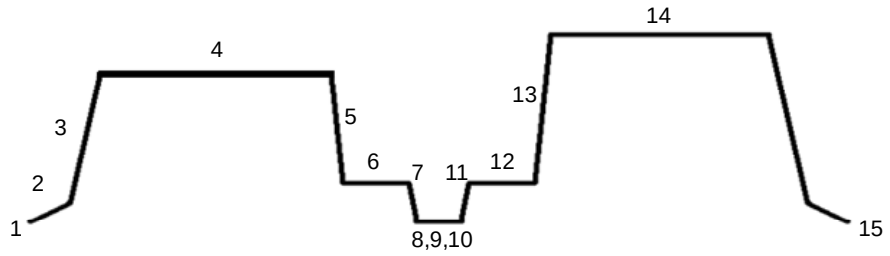

TAKEOFF DIST = 1,930 FT	TOGW = 182,000 LB
BFL = 2,400 FT	INTERNAL FUEL = 39,000 LB
LANDING DIST (AT 7) = 2,080 FT	PAYLOAD = 60,000 LB
MAX ROC@SL,100%WT = 11,300 FT/MIN	WT@80% FUEL = 174,000 LB
FUEL RESERVES (AT 15) = 6.1%	WT@OUTBOUND = 100,000 LB

MISSION SEGMENT	MACH	ALT FT	L/D	FUEL FLOW LB/HR PER ENGINE	TIME MIN	FUEL LB	DIST NM
1. WARM-UP AND TAXI AT IDLE POWER	0	SL	-	2751	8	734	0
2. TAKEOFF AT MAX POWER	0-0.4	SL	-	14763	2	984	0
3. CLIMB TO BCA AT BEST ECONOMIC RATE	0.4-0.6	-	12.6	9808	12	3034	63
4. CRUISE OUT AT BCA	0.8	30,000	11.3	5252	64	11137	500
5. DESCEND TO 1,000 FT	0.8 - 0.6	-	-	-	-	-	-
6. CRUISE AT 1,000 FT	0.6	1,000	6.3	9333	15	4719	100
7. DESCEND TO SEA LEVEL AND LAND	0.6 - 0	SL	-	-	-	347	-
8. DROP PAYLOAD	0	SL	-	-	10	-	-
9. WARM-UP AND TAXI AT IDLE POWER	0	SL	-	2020	8	1212	0
10. TAKEOFF AT MAX POWER	0-0.4	SL	-	18451	2	1228	0
11. CLIMB TO 1,000 FT AT BEST ECONOMIC RATE	0.4-0.6	-	5.9	16637	-	45	0
12. CRUISE AT 1,000 FT	0.6	1,000	3.8	9169	15	4636	100
13. CLIMB TO BCA AT BEST ECONOMIC RATE	0.6-0.8	-	9.9	8088	10	1828	49
14. CRUISE BACK AT BCA	0.8	40,000	9.7	3083	65	6718	500
15. DESCEND TO SEA LEVEL AND LAND	0.8-0	SL	-	-	-	-	-
TOTALS					211	36622	1312

In the combat mission profile the austere transport starts at 182,000 lbs, travels a total distance of 1312 nm in 211 minutes and uses roughly 37,000 lbs of fuel. The aircraft begins its

takeoff at sea level, climbs to 30,000 feet and cruises for 500 nm. It then descends to 1,000 feet and reduces its speed to 0.6 Mach for 100 nm as it nears the drop zone. After the aircraft lands and the payload is removed the aircraft's weight is substantially reduced to 100,000 lbs. At this weight the aircraft can cruise back at an altitude of 40,000 feet which saves thousands of pounds of fuel. The transport will initially carry 39,000 lbs of fuel which leaves 6.1% of fuel reserves.

The transport aircraft will have an operational radius of 656 nm for the combat mission. A great circle mapper tool (Ref 20) was used to illustrate the radius for this configuration and is shown in Figure 3.5 with the initial base being the Virginia Tech Airport (BCB) in Blacksburg, VA.

Figure 3.5 Combat Mission Range Map

The performance characteristics of the ferry mission are shown in Table 3.3 and were found using the same methods as the combat mission however the mission profile and initial weights were different.

Table 3.3 Ferry Mission Profile

Inter-Theater Tactical Transport with Austere STOL Capability FERRY MISSION PROFILE

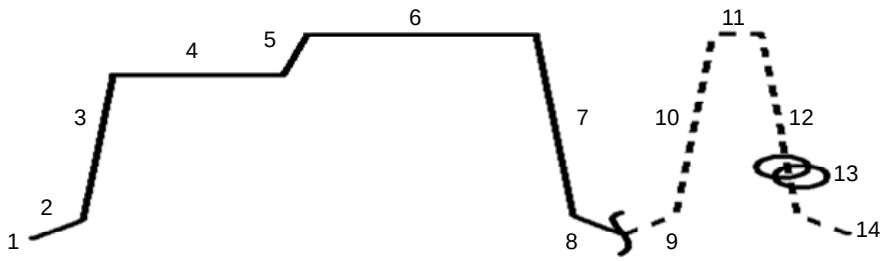

TAKEOFF DIST	= 1,800 FT
BFL	= 2,230 FT
LANDING DIST	= 1,560 FT
MAX ROC@SL,100%WT	= 11,900 FT/MIN
FUEL RESERVES	= ACCOMODATIONS FOR MISSED APPROACH, 150 NM DIVERSION, AND 45 MIN HOLD AT 5,000 FT

TOGW	= 173,000 LB
INTERNAL FUEL	= 39,000 LB
AUX FUEL	= 31,000 LB
PAYLOAD	= 20,000 LB
WT@80% FUEL	= 159,000 LB
WT@MISSED APPROACH	= 112,000 LB

MISSION SEGMENT	MACH	ALT FT	L/D	FUEL FLOW LB/HR PER ENGINE	TIME MIN	FUEL LB	DIST NM
1. WARM-UP AND TAXI AT IDLE POWER	0	SL	-	2751	8	734	0
2. TAKEOFF AT MAX POWER	0-0.5	SL	-	14763	2	984	0
3. CLIMB TO BCA	0.5-0.6	-	12.5	9466	11	2949	63
4. CRUISE OUT AT BCA	0.8	31,000	11.3	4940	194	31986	1520
5. CLIMB TO NEXT BCA	0.6	-	15.8	3588	9	1068	52
6. CRUISE OUT AT NEXT BCA	0.8	40,000	13.1	3307	205	22560	1565
7. DESCEND TO SEA LEVEL	0.8-0	-	-	-	-	-	-
8. LAND, TAXI, AND PARK	0	SL	-	1184	10	395	0
9. TAKEOFF AT MAX POWER (MISS APP)	0-0.5	SL	-	20655	2	1377	0
10. CLIMB TO BCA	0.5	-	10.9	8149	12	2325	64
11. CRUISE OUT AT BCA (DIVERSION)	0.8	40,000	11.0	3183	20	2081	150
12. DESCEND TO 5,000 FT	0.8-0.2	SL	-	-	-	-	-
13. HOLD FOR 45 MIN AT 5,000 FT	0.2	5,000	15.5	1973	45	2959	0
14. DESCEND TO SEA LEVEL AND LAND	0.2-0	SL	-	-	-	-	-
TOTALS					518	69418	3414

The ferry mission begins at a TOGW of 173,000 lbs with 70,000 of those pounds being solely fuel. The internal volume of the transport's wing was found to have sufficient space for this amount of fuel; this saves the need for aerial refueling in our design. The aircraft has a staged climb halfway through its cruise segment to a higher altitude in order to conserve fuel while flying at a lower weight. The initial cruise is at an altitude of 31,000 feet then is transitioned to 40,000 feet after 1600 nm. Once the aircraft reaches its 3200 nm destination it still needs reserve fuel for a missed approach, a 150 nm diversion, and a 45 minute hold at 5,000 feet. The dashed segments (numbers 9 – 14) on Table 3.3 represent the reserve fuel requirements. With the diversion the aircraft travels a total distance of 3414 nm in 518 minutes or approximately 8 and one half hours.

If the aircraft were to be ferried from the Virginia Tech Airport and knowing that the engines being used on this design have a 180 minute ETOPS rating the range on a great circle map would be as shown below in Figure 3.6 and was produced from Swartz (Ref 20).

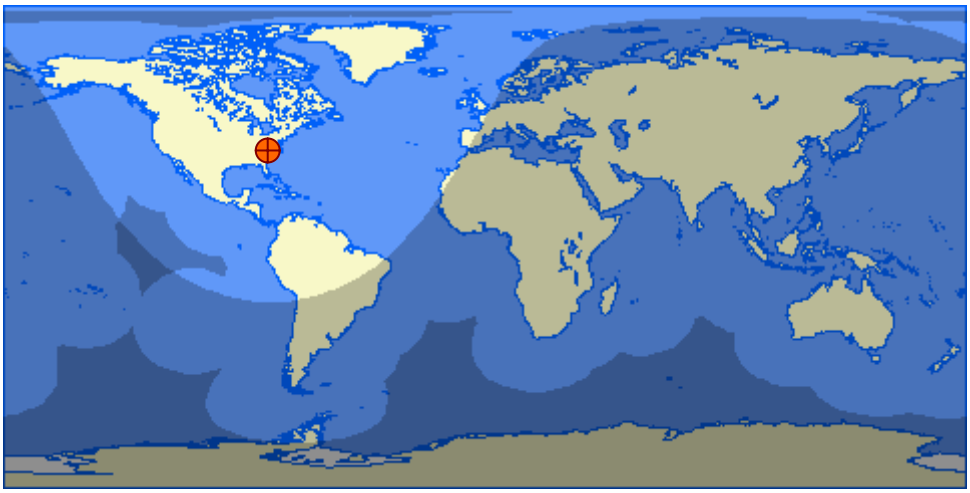

Figure 3.6 Ferry Mission Great Circle Map with 180 Min. ETOPS

3.3 TAKEOFF

The RFP requires the austere transport to takeoff with a balanced field length of 2,500 ft on a hot day. The Skymaster II has a balanced field length of 2,380 feet. This short takeoff is made possible by the high thrust to weight ratio (0.42) and an externally blown flap system that is expected to generate a C_{Lmax} of at least 4.0. The takeoff distance for the austere transport was calculated using a methodology of a proposal by Krenkal and Salzman (Ref 18). Their method included the aircraft equations of motion for ground roll and climb. However a rotation phase and a balanced field length calculation based on one engine inoperative (OEI) takeoff was developed. Krenkal and Salzman's methodology relied on the balance of force equations during the ground roll and climb segments. Ground roll was obtained by summing the forces on the aircraft in the horizontal direction given by Equation 3.1.

$$\frac{du}{dt} = \frac{g}{W}\left[T\cos\Lambda - 0.5\rho S C_D u^2 - \mu\left(W - 0.5\rho S C_L u^2 - T\sin\Lambda\right)\right] \qquad \text{Eq. 3.1}$$

The climb phase is given by four equations where the first two are the balance of force equations (Equations 3.2 and 3.3), a third relates velocity to the climb angle, γ (Equation 3.4), and the fourth a total velocity V (Equation 3.5).

$$\frac{du}{dt} = \frac{g}{W}\left[T\cos(\Lambda+\gamma) - 0.5\rho S\left(C_L\sin\gamma + C_D\cos\gamma\right)V^2\right] \qquad \text{Eq. 3.2}$$

$$\frac{du}{dt} = \frac{g}{W}\left[T\sin(\Lambda+\gamma) + 0.5\rho S\left(C_L\cos\gamma + C_D\sin\gamma\right)V^2 - W\right] \qquad \text{Eq. 3.3}$$

$$\tan\gamma = \frac{v}{u} \qquad \text{Eq. 3.4}$$

$$V = \left(u^2 + v^2\right)^{\frac{1}{2}} \qquad \text{Eq. 3.5}$$

The FAR 25 takeoff velocity requirements are given by

$$V_r \geq 1.05 V_{MC} \qquad \text{Eq. 3.6}$$

$$V_{lo} \geq 1.1 V_{MU} \qquad \text{Eq. 3.7}$$

$$V_2 \geq 1.2 V_{MC} \qquad \text{Eq. 3.8}$$

With V_r being the rotation speed, V_{lo} the speed at liftoff, and V_2 the speed once the aircraft has cleared the 50 ft high obstacle at the end of the runway. V_{MC} is the minimum control velocity which is the slowest speed that the aircraft can fly with one engine inoperative. The minimum unstuck velocity, V_{MU}, is close to the stall speed of the aircraft given by

$$V_{stall} = \sqrt{\frac{2(W/S)}{\rho C_{L\max}}} \qquad \text{Eq. 3.9}$$

Since the stall speed is easier to determine than V_{MU} it was used to calculate the initial rotation speed.

For OEI requirements FAR 25 defines a new takeoff speed V_1 where $V_r \geq V_1$ and $V_{lo} \geq 1.05 V_{MU}$. V_1 is the decision velocity where the pilot must either continue taking off with

OEI or break to a full stop and abort takeoff. The balanced field length was found from iterating a solution where takeoff over a 50 ft obstacle was equal to the stopping distance of the aircraft. The stopping distance was calculated by summing braking force with zero thrust in the horizontal direction.

The first takeoff in the combat mission is the most critical takeoff distance since the aircraft is at its heaviest 182,000 lbs. It is fully loaded with fuel and 60,000 lb payload and is assumed to be operating on a hot day. Table 3.4 summarizes each of the takeoff analyses for the combat and ferry missions. The first takeoff of the combat mission is 182,000 lbs; the second takeoff is 100,000 lbs. The ferry mission takes off at 173,000 lbs.

Table 3.4 Takeoff Analysis

	Combat Takeoff #1	Combat Takeoff #2	Ferry Takeoff	
Weight	182,000	100,000	173,000	(lbs)
Rotation Velocity	157.4	116.7	153.4	(ft/s)
Liftoff Velocity	195.4	188.2	193.6	(ft/s)
Velocity Over Obstacle	201.4	195.4	199.9	(ft/s)
Rotation Distance	963.1	281.6	867.1	(ft)
Liftoff Distance	1492	739.2	1388	(ft)
Distance to Obstacle	1928	980.4	1800	(ft)
Rotation Time	12.20	4.82	11.27	(sec)
Liftoff Time	15.20	7.82	14.27	(sec)
Time to Obstacle	17.40	9.12	16.37	(sec)
TOTAL TAKEOFF DIST	1928	980.4	1800	(ft)
TOTAL TAKEOFF TIME	17.40	9.115	16.37	(sec)
BFL	2380	1217	2230	(ft)

3.4 LANDING

The RFP requires the STOL transport to land on a blacktop (CBR 4-6) with a 3000 foot by 150 foot useful area with 50 foot obstacles at 250 feet from either end of the runway. Due to the nature of a combat situation the airfield may also be oriented in a less than optimal direction

therefore the aircraft must be designed to land in a 5 knot tailwind component. The Skymaster II has a landing distance of 2080 feet at the drop zone airfield and includes the approach over the 50 foot obstacle. The aircraft would be landing with a weight of approximately 161,000 lbs. Special consideration was given to the CBR of the runway and is discussed at length in the landing gear section.

The landing analysis was broken into three sections: the approach, the flare, and the ground roll (which includes a free roll period and a breaking distance). Below in Figure 3.7 is an illustration of the phases of landing.

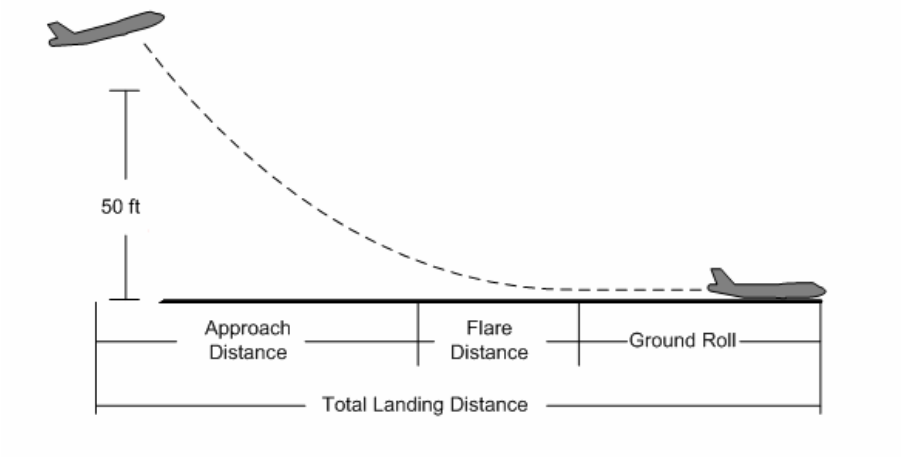

Figure 3.7 Three Phases of Landing Used in Calculating Landing Distance

The aircraft approaches at angle γ and is found by

$$\gamma = \arcsin\left(\frac{T}{W} - \frac{1}{L/D}\right) \qquad \text{Eq. 3.10}$$

The approach angle for conventional transports is typically 3 degrees, however with a STOL transport larger approach angles could be expected and was found to range from 4 to 5 degrees. The average velocity during flare is $1.15V_{stall}$ for military aircraft. The flare radius can be found from flare velocity, V_f, and n from

$$R = \frac{V_f^{\,2}}{g(n-1)} \qquad \text{Eq. 3.11}$$

The velocity at touchdown is determined from $1.1V_{stall}$ for military aircraft. The ground roll distance is calculated from summing horizontal forces for a period of no braking to a period of braking and reverse thrusting. The Skymaster II will make use of reverse thrusters which were assumed to provide at least 30% of the maximum forward thrust. Table 3.5 summarizes the landing distances of the aircraft in both the combat and ferry mission configurations.

Table 3.5 Landing Analysis

	Combat Landing #1	Combat Landing #2	Ferry Landing	
Weight	161,000	86,000	113,000	(lbs)
Stall Speed	138.5	103.5	117.4	(ft/s)
Approach Speed	166.2	124.2	140.9	(ft/s)
Touchdown speed	152.4	113.9	129.2	(ft/s)
Vertical Speed	10.7	10.3	9.9	(ft/s)
Approach Angle	4.0	5.2	4.4	(deg)
Approach Distance	685.4	529.1	627.5	(ft)
Flare Distance	55.2	40.0	43.5	(ft)
Free Roll Distance	304.8	227.8	258.4	(ft)
Braking Distance	1031.5	423.4	631	(ft)
TOTAL LANDING DISTANCE	2076	1220	1560	(ft)

In the above table the three different weights are shown for the landing at the drop zone airfield (161,000 lbs), the landing after the aircraft returns to base from the combat mission (86,000 lbs), and the ferry mission landing (113,000 lbs). The vertical speeds of the aircraft when landing on the runway are also noted and are within the STOL suggested 15 ft/s sink speed as noted in Raymer (Ref 2).

3.5 CLIMB

The rate of climb of the Skymaster II is given below in Figure 3.8. The maximum rate of climb is the least time to gain altitude. It is shown in solid lines and is 11,300 feet per minute at TOGW and sea level conditions for the STOL transport. As the weight decreases climb rate

increases and as the altitude increases climb rate decreases. The maximum angle of climb is shown in dashed lines and is substantially less with a rate of climb at 5,000 feet per minute at TOGW and sea level conditions. The service ceiling climb rate is shown in purple at 500 feet per minute. With the fully loaded aircraft this ceiling is at 41,000 feet which beats the RFP requirement of 30,000 feet.

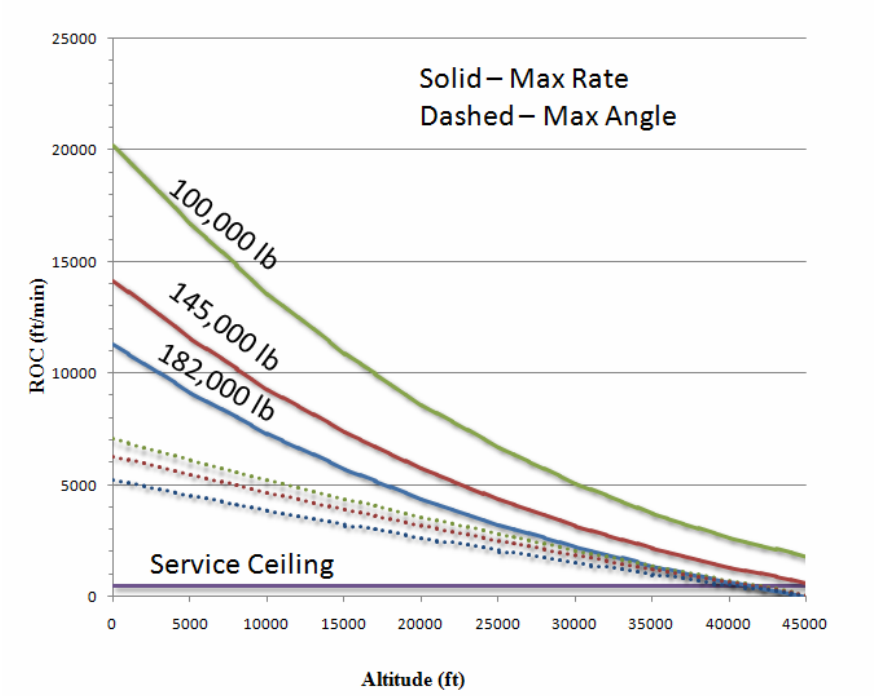

Figure 3.8 Rate of Climb for Various Weights (Max Rate and Max Angle of Climb)

The climb calculations were computed using Marchman (Ref 6). The maximum rate of climb (dh/dt) C_L is defined from Eq. 3.12.

$$C_{L\max\frac{dh}{dt}} = \frac{-\frac{T}{W} \pm \sqrt{(T/W)^2 + 12C_{D0}K}}{2K} \qquad \text{Eq. 3.12}$$

Where thrust, T is constant. The speed in climb is found from

$$V = \sqrt{\frac{2W}{\rho S C_L}} \qquad \text{Eq. 3.13}$$

And the angle of maximum rate of climb is given by

$$\sin\theta = \frac{T}{W} - \frac{C_D}{C_L} \qquad \text{Eq. 3.14}$$

The rate of climb, dh/dt is then equal to the velocity (Eq. 3.13) times the sin of climb angle (Eq. 3.14).

The maximum angle of climb which is defined as the least distance traveled to gain altitude is found from approximating a C_L at minimum drag conditions. The maximum angle of climb for the austere STOL transport is 21.8 degrees.

4 AERODYNAMICS

A study of velocity at minimum drag was done at different altitudes by using the parabolic drag polar equation below.

$$D = C_{D0}\frac{1}{2}\rho V_\infty{}^2 S + 2KW^2 / \rho S V_\infty{}^2 \qquad \text{Eq. 4.1}$$

The plot below in Figure 4.1 shows the effect of altitude on drag variation. It should be noted that wave drag was excluded from this chart as it would have no effect on what the minimum drag velocity is for any given altitude.

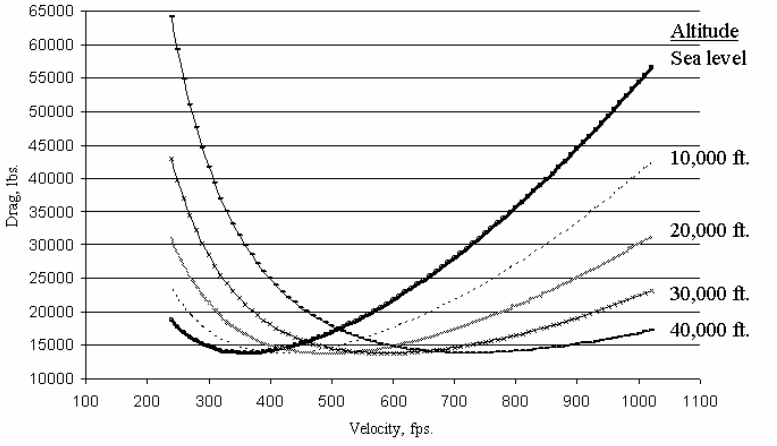

Figure 4.1: Drag vs. Velocity at Varying Altitude

From the figure above the minimum drag is about 12730 pounds at every altitude, but the problem is flying at the speed where this occurs. The RFP sets the cruise speed at Mach 0.8 or 796 fps at an altitude of 30,000 feet. However, for our concept the minimum drag at 30,000 feet is found at a velocity of 600 fps. To cruise at Mach 0.8 at minimum drag conditions the aircraft would have to fly at 40,000 feet as shown from the figure. Since our concept has a high $(L/D)_{max}$ it allows for less drag so that even if the concept aircraft was not flying at minimum drag velocity it would still be less drag than another lower $(L/D)_{max}$ aircraft which is flying at its minimum drag condition. The minimum drag velocity was also studied for different aircraft configurations by varying wing area and aspect ratio to see where our aircraft would cruise in relation to the minimum drag point.

Even though the concept aircraft will not cruise at minimum drag it is still acceptable since the amount of drag is much smaller for a high $(L/D)_{max}$ aircraft as has been stated before. The 30,000 feet is an acceptable cruising altitude given the requirements of the RFP and the fact that there is about 3200 pounds of more thrust available at this altitude than 40,000 feet based on the engine that has been chosen.

4.1 CRUISE DRAG

Drag calculations were done using a friction and form drag code *FRICTION* (Ref 24). This code was modified using the Raymer method (Ref 2) to include induced drag, wave drag, and trim drag as well as miscellaneous drag resulting from components of the aircraft such as the rear upsweep and the windshield. This method includes skin friction coefficients, Reynolds number, wetted surface area, Mach number, and altitude inputs to determine each component of the drag coefficient for the aircraft. Leakage and protuberances were calculated to be approximately 2% of the overall drag, and is included in the miscellaneous drag.

By implementing struts in the design, the span of the wing could be increased which increases the aspect ratio, and thereby reducing the total drag of the aircraft. This, combined with the weight savings offered by the strut-braced wing design, reduced the parasite and induced drag a considerable amount. The parasite drag was reduced drastically due to the higher aspect ratio wing, and the induced drag was reduced a substantial amount due to the fact that a much lower C_L of 0.3 can be used in cruise. The Figure 4.2 shows how the strut is beneficial:

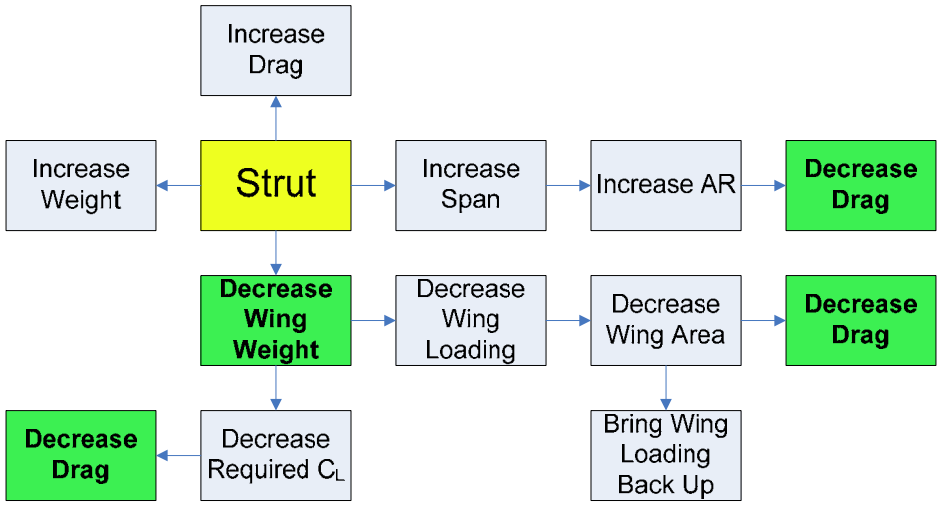

Figure 4.2: Benefits of a Strut-braced Wing Configuration

Analysis was done for a cantilevered wing of the same span and planform area. To keep the same planform, the wing would need to be twice as thick if it did not have the support of the strut. This would increase the form drag by over twenty counts. More importantly, it would significantly increase the wave drag. If the wing needed to be twice as thick as it is, the cruise drag for the aircraft would be insurmountable. The savings in drag and weight with use of the strut outweigh the drag and weight created by the strut itself on the aircraft.

One of the major components of a military transport aircraft is the rear upsweep of the plane. This is angle between the centerline of the fuselage and the top of the rear of the plane, measured from the point where the upsweep begins.

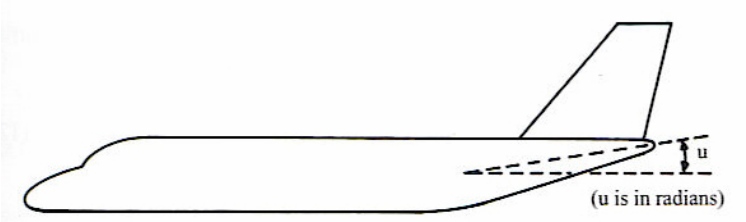

Figure 4.3: Upsweep Angle Visualization (Ref 2)

The upsweep drag component is calculated using the equation below

$$\frac{D}{q}_{upsweep} = 3.83u^{2.5}A_{\max} \qquad \text{(Ref 2)} \qquad \text{Eq 4.2}$$

and then dividing by the wing reference area.

Current loading methods require this area to be relatively large, and fairly flat. If the angle of the upsweep is too abrupt, major losses in cruise performance are suffered due to pressure drag. It can be seen in Figure 4.7 that the miscellaneous section of the drag coefficient is already a fairly substantial contributor to the overall drag of the aircraft. Because of this, the boom tail design was quickly eliminated, and great care was taken to minimize the abruptness of the upsweep on the Skymaster II. It was found that an upsweep angle of 13° is sufficient for both loading and cruise performance requirements.

In addition to struts and minimization of upsweep to reduce drag, an efficient span load distribution is desired. Using *LAMDES*, a Lamar Design Optimization code, a proper span wise twist distribution was calculated to achieve the appropriate span load. Figure 4.4 below shows the twist distribution required to achieve our desired span load efficiency at our design cruise C_L of 0.3.

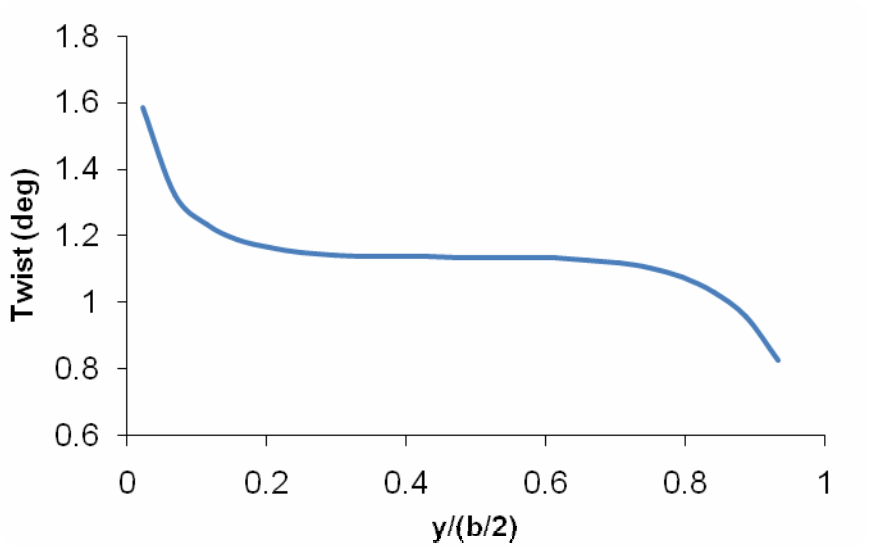

Figure 4.4: Span wise Twist Distribution

Because the cruise requirements for the Skymaster II call for a minimum cruise speed of Mach 0.8, it is important to minimize wave drag as much as possible. For this purpose, a supercritical airfoil was selected, with a 12% thickness to chord ratio. The supercritical airfoil offers various characteristics desirable for transonic flight. The rounded leading edge and reduced slope on the upper surface help to weaken the existing shock wave, thus reducing the wave drag. The particular airfoil used for this aircraft is the NASA Supercritical SCW-2a. A pressure distribution analysis was done using *TSFOIL* developed by Earl Murman (Ref 23) at NASA Ames. Its pressure distribution at cruise conditions for a wing with a leading edge sweep of 15° is shown below in Figure 4.5. For the required flight conditions, this airfoil creates a fairly weak shock at approximately 60% chord as to not interfere with the control surfaces, as well as the required lift in the aft section of the wing. This creates the desired shock strength and, when coupled with the high lift system, provides the C_L values needed for takeoff and landing.

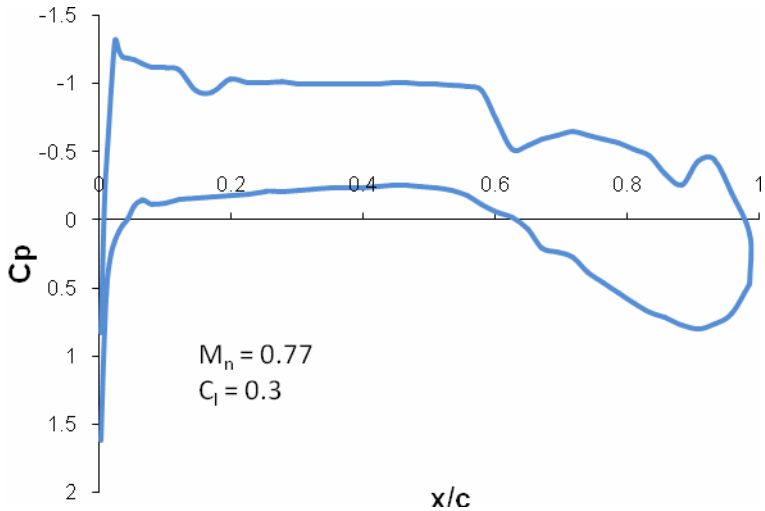

Figure 4.5: Pressure Distribution

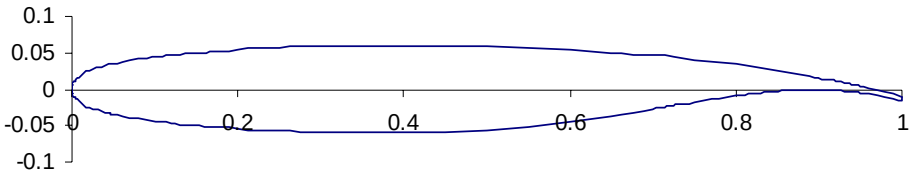

Figure 4.6: NASA SCW-2a Airfoil

The drag build up for the Skymaster II was calculated at an altitude of 30,000 feet. In Figure 4.7 below, the drag coefficient for each component of the aircraft at cruise is shown, including the overall drag due to lift as well as the wave drag up to a cruise Mach number of 0.9 to account for the transonic drag rise that will be experienced. Figures 4.8 and 4.9 show the drag build up for takeoff and landing respectively. As shown from the graphs, the drag at takeoff and landing is dominated by induced drag due to their high C_L values, especially at takeoff. It is important to note that the miscellaneous section of these charts is comprised of the drag due to upsweep, the windshield, and the leakages and protuberances such as pitot tubes, door handles, air refueling couplings, etc.

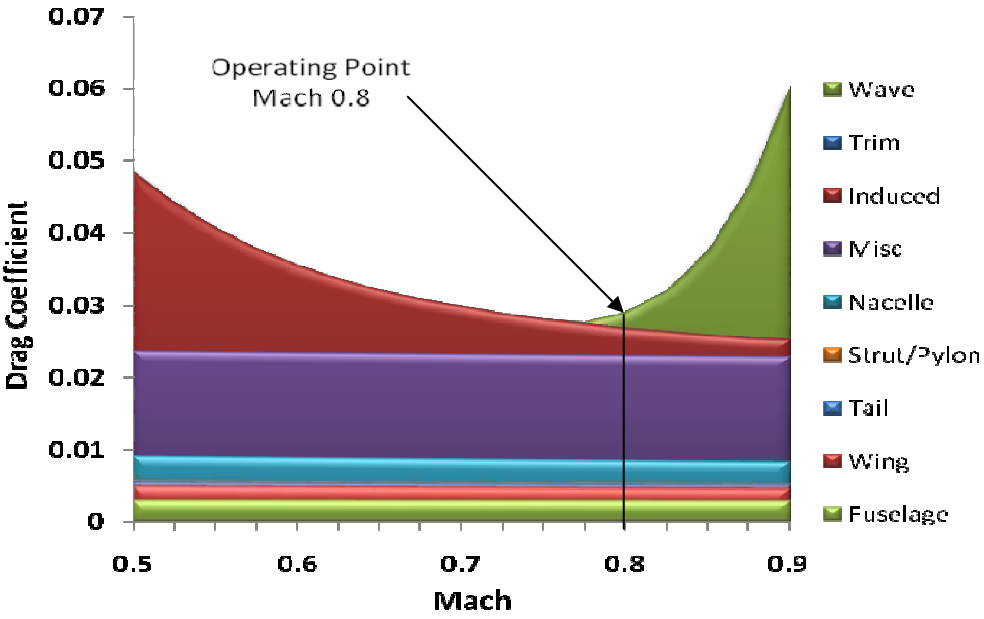

Figure 4.7: Cruise Drag Buildup

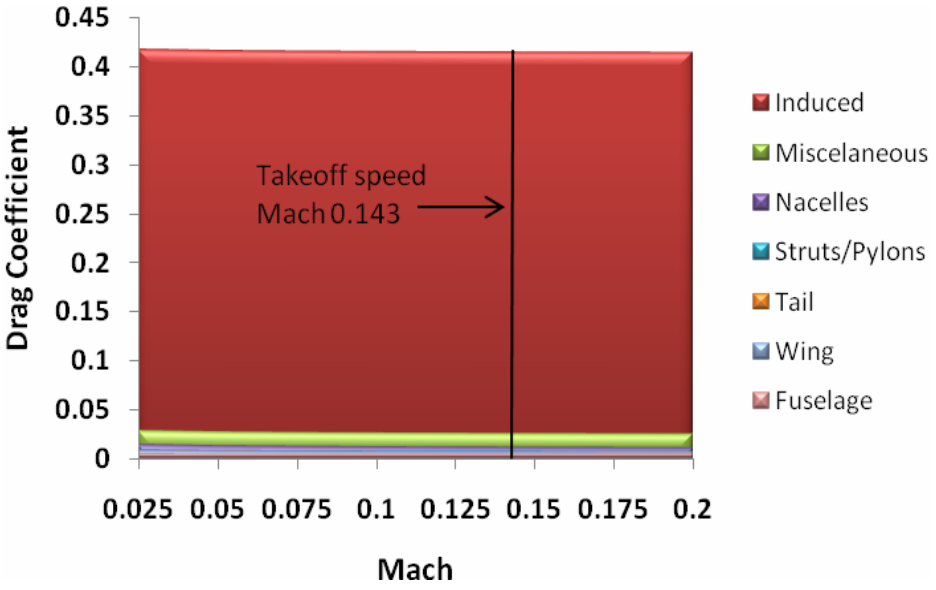

Figure 4.8: Takeoff Drag Buildup

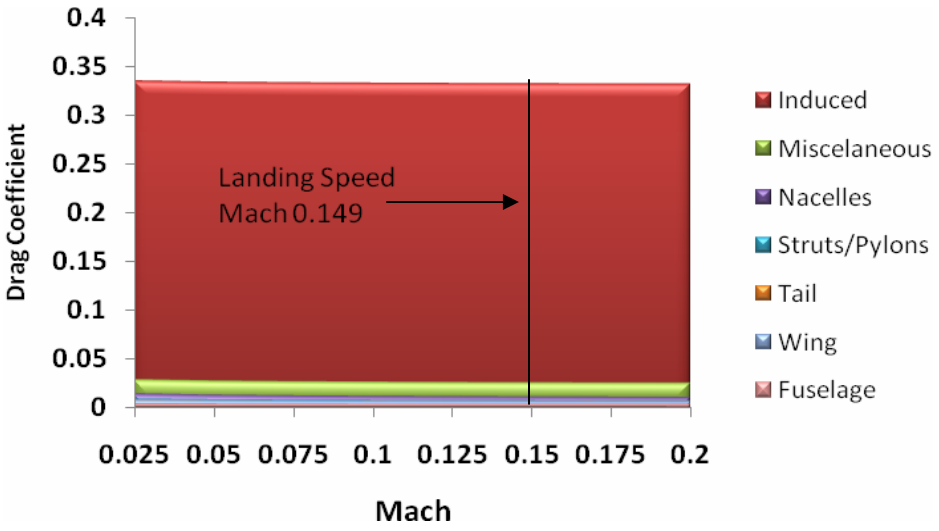

Figure 4.9: Landing Drag Buildup

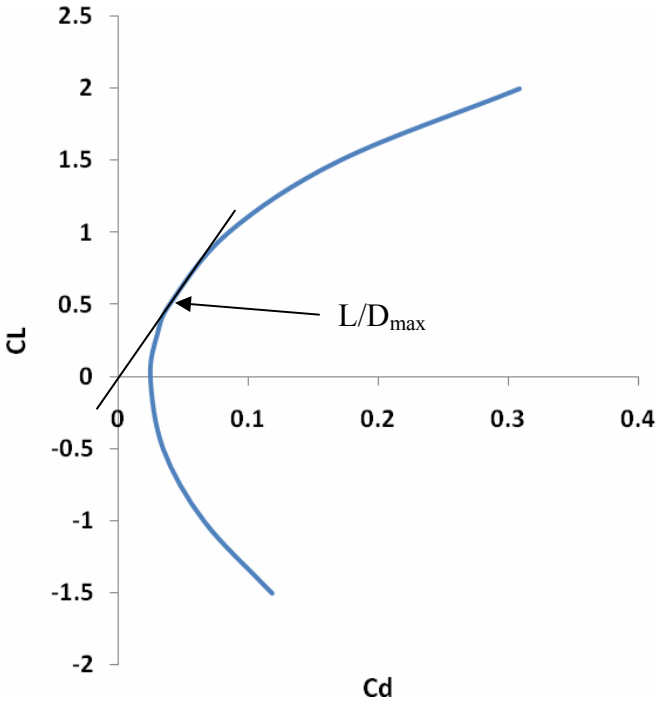

Figure 4.10: Cruise Drag Polar

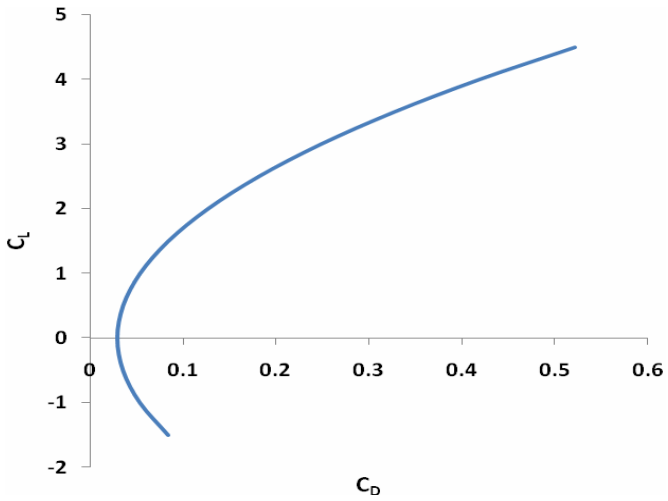

Figure 4.11: Takeoff Drag Polar

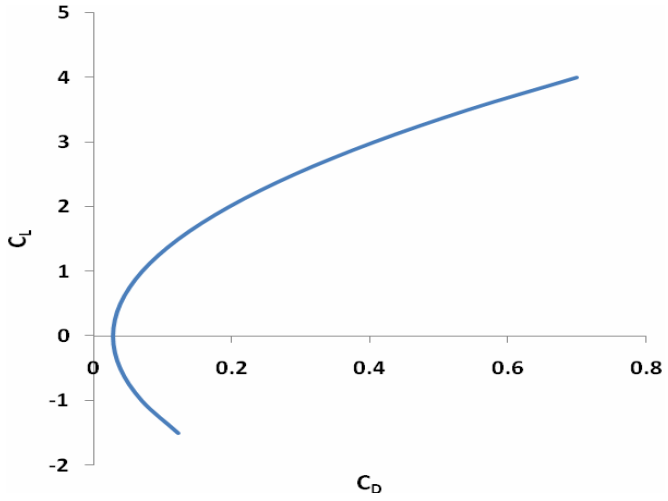

Figure 4.12: Landing Drag Polar

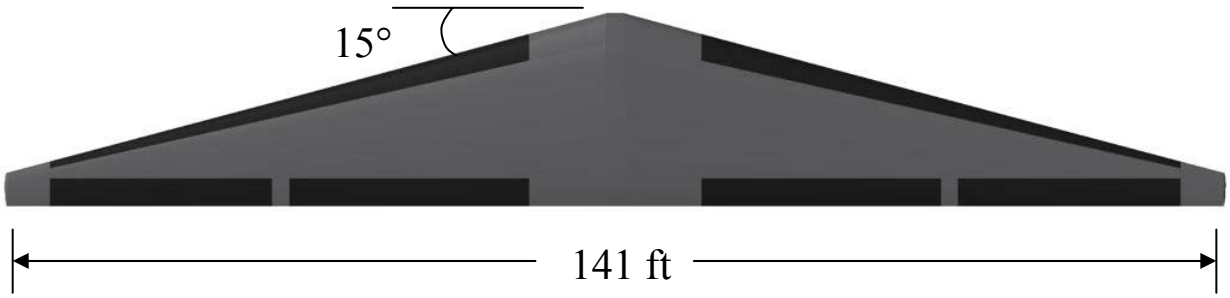

Figure 4.13: Wing Planform

4.2 HIGH LIFT SYSTEM

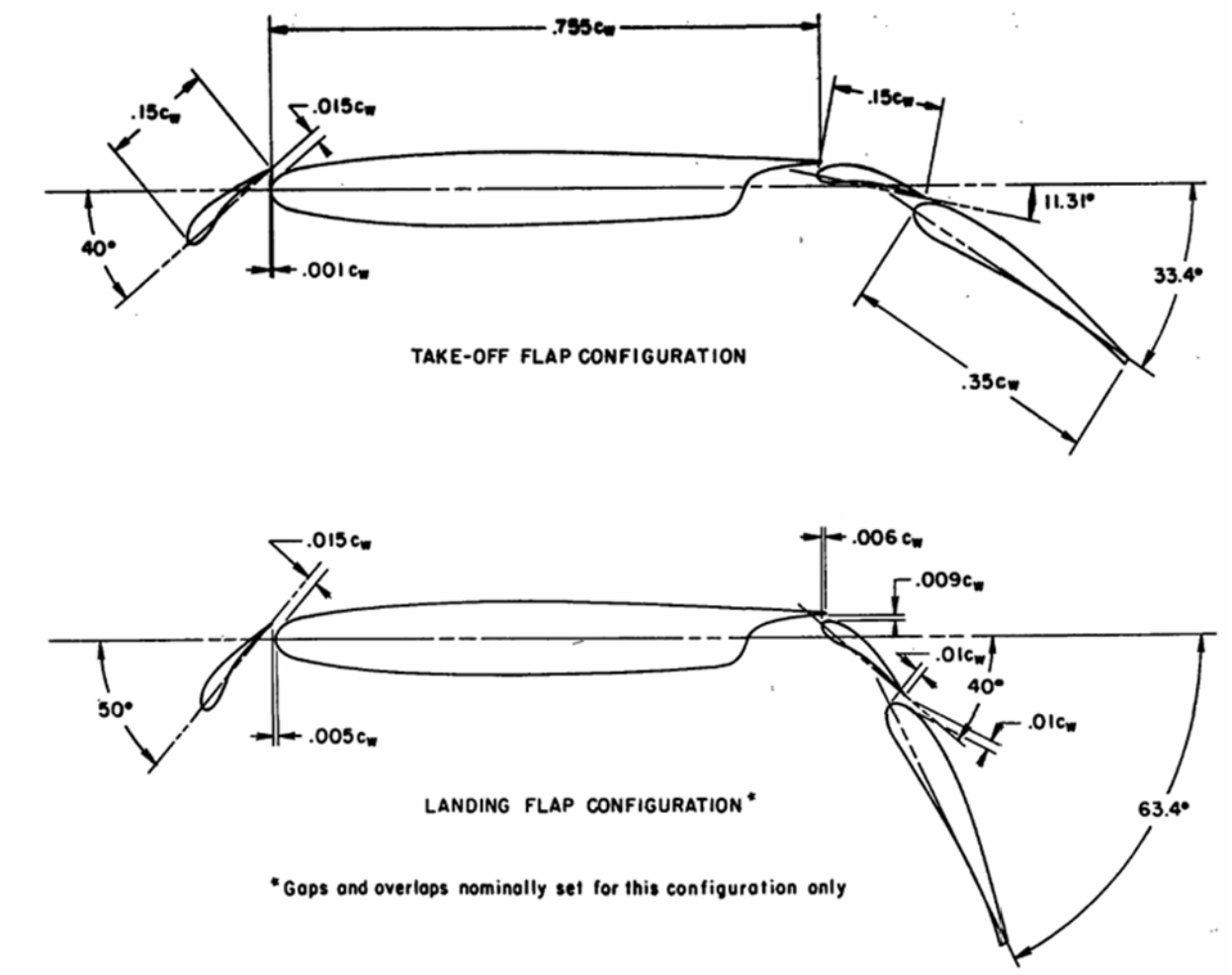

Figure 4.14: High-lift system dimensions and configurations (Ref. 19)

Based on the takeoff analysis, a lift coefficient of 4.0 is needed to takeoff within 2500 feet as required by the RFP. To achieve the high lift required the use of Externally Blown Flaps (EBF) is incorporated into the design of the Skymaster II. Typical estimates of the maximum lift coefficient for EBF aircraft are in the range of 3 to 8. As there is currently no reliable computational method for estimating the performance of an externally blown flap system, wind tunnel data is used to estimate the maximum lift coefficient attainable.

In the 1970s, NASA conducted an investigation to determine the low-speed aerodynamic characteristics of a four-engine, swept-wing, jet-powered STOL transport with externally blown

flaps. The model was tested using air ejectors to simulate engines having a bypass ratio of 6.2 mounted on pylons under a 9.3-percent-thick supercritical airfoil wing (Ref. 19). The Skymaster II has a thicker airfoil section and a significantly smaller wing sweep than the NASA model, which would imply that the Skymaster II lift coefficient obtained would be somewhat higher than that predicted using the wind tunnel data. A comparison of the planform areas of the Skymaster II and the wind tunnel model can be seen in Figure 4.15.

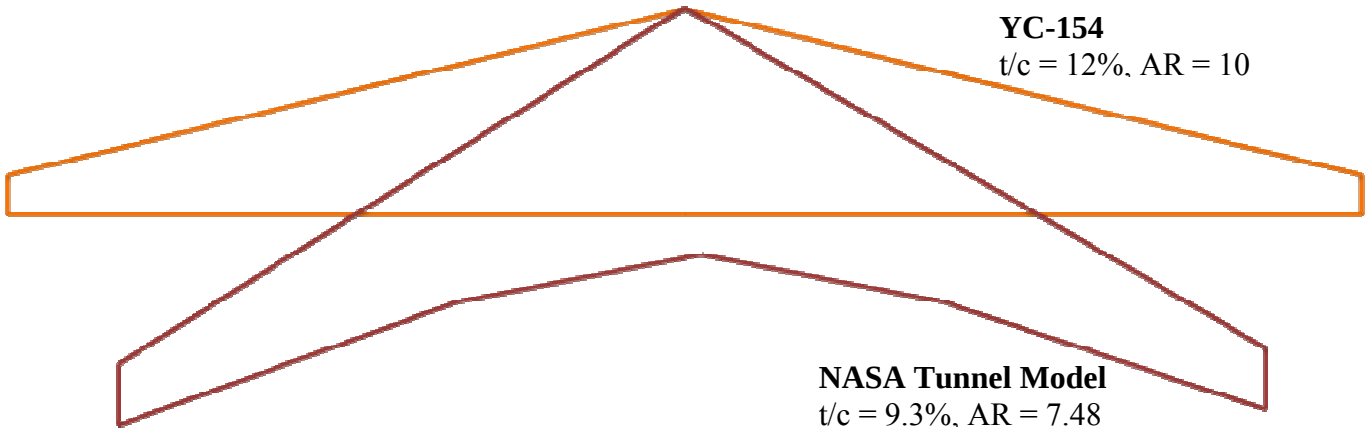

Figure 4.15: Comparison of YC-154 Planform Area to NASA Wind Tunnel Model (Ref 19)

The maximum lift coefficient was determined by interpolating between lift-curves plotted for different thrust coefficients. The thrust coefficient C_T is defined as,

$$C_T = T/qS \qquad \text{Eq. 4.3}$$

where T is the total gross thrust, q is the free stream dynamic pressure, and S is the wing area. For takeoff and landing, the thrust coefficient is 1.01 and 0.71 respectively. The thrust coefficient for landing is lower due to the reduced power setting. Figure 4.16 shows that the maximum lift achieved for takeoff is $C_{L,max} = 4.0$. The takeoff configuration has a flap deflection of 35 degrees and a slat deflection of 50 degrees. Figure 4.17 shows that $C_{L,max} = 3.9$ for the landing configuration which has a flap deflection of 65 degrees and a slat deflection of 50 degrees. Once

again, the Skymaster II will have slightly larger maximum lift coefficients due to the thicker airfoil and smaller wing sweep than the model. With the SCW-2a, a 12% thick airfoil, and a leading edge sweep of 15°, the wing configuration of the Skymaster II is estimated to be capable of attaining a C_{Lmax} of at least, but likely greater than, 4.0. The maximum lift coefficients obtained are based on the flap system pictured in Figure 4.14. The takeoff configuration has a smaller flap deflection so that drag is lower during takeoff.

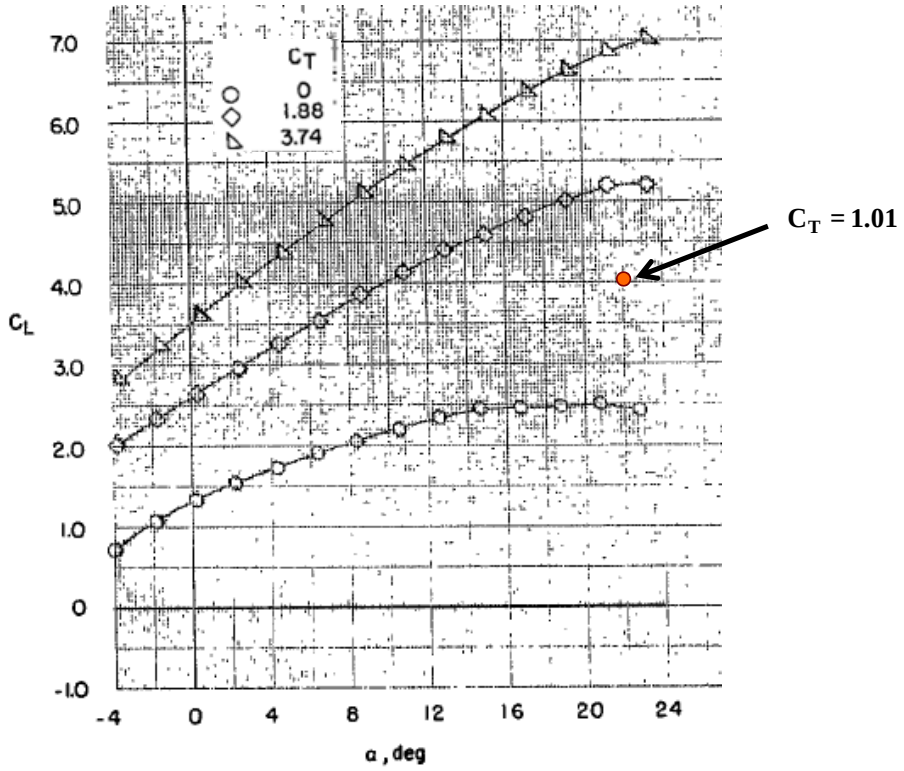

Figure 4.16: NASA Wind Tunnel Data for Takeoff Configuration δ_f = 35° and δ_s = 50° (Ref. 19)

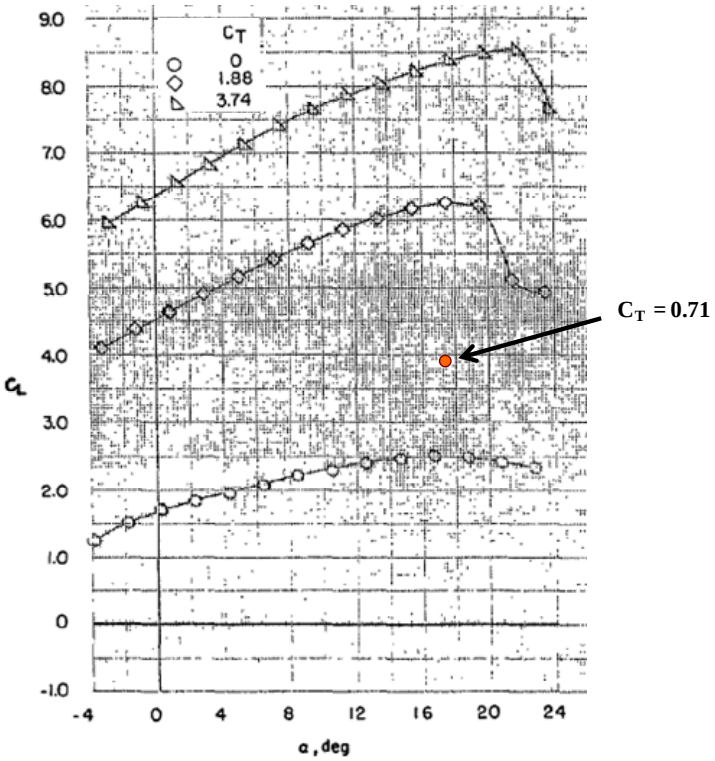

Figure 4.17: NASA Wind Tunnel Data for Landing Configuration $\delta_f = 65^\circ$ and $\delta_s = 50^\circ$ (Ref. 19)

5 PROPULSION

5.1 ENGINE SIZING

For a TOGW of 182,000 pounds and a Thrust-to-Weight ratio of 0.42, the amount of thrust needed per engine for a two engine aircraft is approximately 39,000 pounds. The choice to use two engines was made for many reasons. The maintenance required for two engines is lower, reducing life cycle costs. In addition, the wetted area of the engines is lower causing a reduction in drag. High-bypass ratio turbofan engines were considered since they are more efficient than low-bypass ratio turbofans and pure turbojets at subsonic speeds.

Installation effects were examined to determine the uninstalled thrust. The effect from inlet pressure recovery is estimated using the equation from Raymer (Ref 2)

$$\%\ \text{thrust loss} = C_{ram}\left[\left(\frac{P_1}{P_0}\right)_{ref} - \left(\frac{P_1}{P_0}\right)_{actual}\right] \times 100 \qquad \text{Eq 5.1}$$

where the "ram recovery correction factor" C_{ram} is approximated at 1.35, $\left(\frac{P_1}{P_0}\right)_{ref} = 1.0$ for subsonic flight, and $\left(\frac{P_1}{P_0}\right)_{actual} = 0.98$ for a subsonic podded nacelle. The resulting thrust loss due to inlet pressure recovery is 2.7 percent. In addition, the losses from the bleed air extracted were estimated using the following equation from Raymer

$$\%\ \text{thrust loss} = C_{bleed}\ (\%\ \text{bleed flow required}) \qquad \text{Eq 5.2}$$

where C_{bleed} is the "bleed correction factor" and is approximated at 2.0. The bleed flow required typically ranges from 1-5% and is assumed to be 3% for initial studies. This results in a 6% loss in thrust due to bleed air extraction alone. Horsepower extraction was ignored since it usually has only a small effect upon installed thrust. Also, installation effects from the nozzle were not included since it is rare to use a nozzle other than that provided by the manufacturer (Ref 2). The resulting uninstalled static thrust needed is approximately 42800 pounds and is the value used to consider off-the-shelf engines.

5.2 Engine Selection

Four existing engines: the Pratt & Whitney F117-PW-100 (PW2043), the Rolls-Royce RB211-535, the GE CF6-6, and the GE/SNECMA CFM56-5C were considered in addition to the AIAA BPR 6 engine. Table 5.1 below compares the thrust, SFC, and dimensions of each engine and provides the scale factor, defined as the thrust required divided by thrust available, necessary for each engine.

Table 5.1: Engine Comparison

Engine	Bypass ratio	Maximum uninstalled thrust (lb)	Inlet diameter (in)	Maximum diameter (in)	Length (in)	Weight (lb)	Cruise SFC (lb/lb/hr)	Scale Factor
F117-PW-100	**5.9**	**43000**	**78.5**	**84.5**	**146.8**	**7100**	**0.563**	**0.99**
RR RB211-535	4.3	43100	74.1	85.2	117.9	7264	0.598	0.99
AIAA BPR 6	6.0	42046	82.1	94.4	128.1	7891	0.610	1.02
GE CF6-6	5.7	41500	86.4	105	183	8176	0.564	1.03
CFM56-5C	6.4	34000	72.3	83.1	103.0	5494	0.567	1.26

The preferred engine is the Pratt & Whitney F117 for multiple reasons. First, the current engine nearly matches the thrust required. Second, the F117 has the lowest cruise SFC. Third, the Pratt & Whitney has a lower weight than the GE CF6, RR RB211 and the AIAA engine. Additionally, the F117 is the only engine that has both bypass and core cascade thrust reversers as shown in Figure 3.19. Furthermore, the PW2043 has 180-minute ETOPS approval, a necessity since the aircraft has only two engines. Finally, the Air Force is familiar with the Pratt & Whitney engine which powers the highly successful C-17 Globemaster III. The CFM56 was not chosen because of the 26% scale factor, although a scaled CFM56 would have a weight and SFC similar to the F117.

5.3 THE F117-PW-100 ENGINE

Although the F117 has a thrust rating listed at 40,400 pounds, it will be upgraded to 43,000 pounds through "minor external modifications" by Pratt and Whitney (Ref. 3). In addition, the engines will be tailored to meet the bleed air demands of the environmental control system (ECS) and the onboard inert gas generating system (OBIGGS) in the event of one engine inoperative. Table 5.2 shows some key performance measures and dimensions of the engine. Figure 5.1 displays the installed thrust available versus Mach number at various altitudes. The

specific fuel consumption (SFC) is plotted versus Mach number for various altitudes in Figure 5.2.

Table 5.2: F117-PW-100 Engine Statistics

F117-PW-100 Engine	Value
Uninstalled thrust (lb)	43000
SL installed takeoff thrust (lb)	39329
Mach 0.8, 30k ft cruise thrust (lb)	8572
SL reverse thrust (lb)	11799
Inlet diameter (ft)	6.54
Maximum diameter (ft)	7.04
Length (ft)	12.23
Weight (lb)	7100
Weight flow (lb/s)	1323

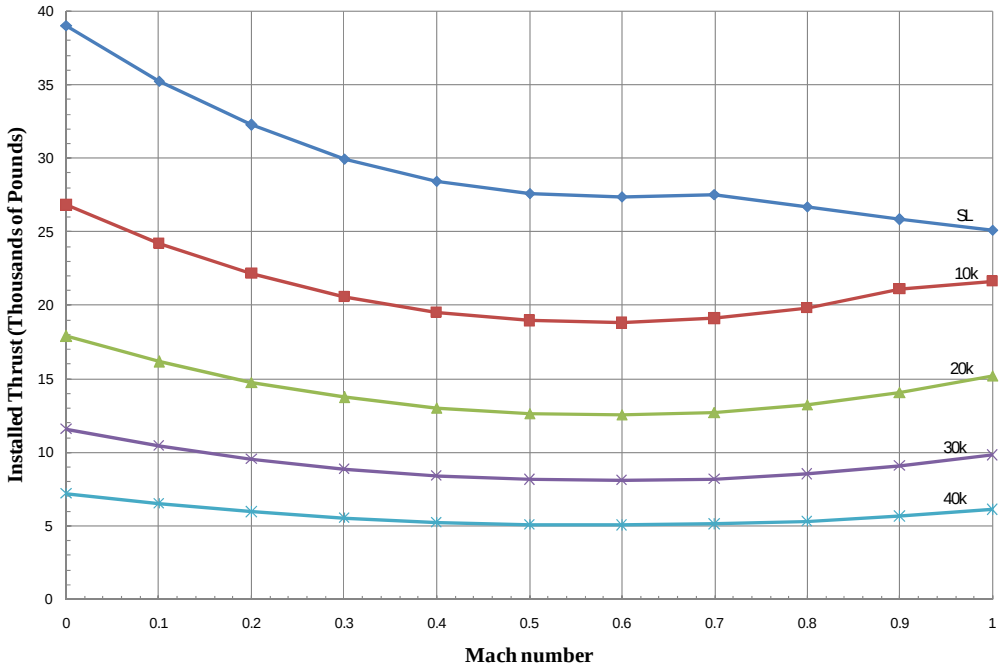

Figure 5.1: Installed Thrust versus Mach Number at Maximum Continuous Power

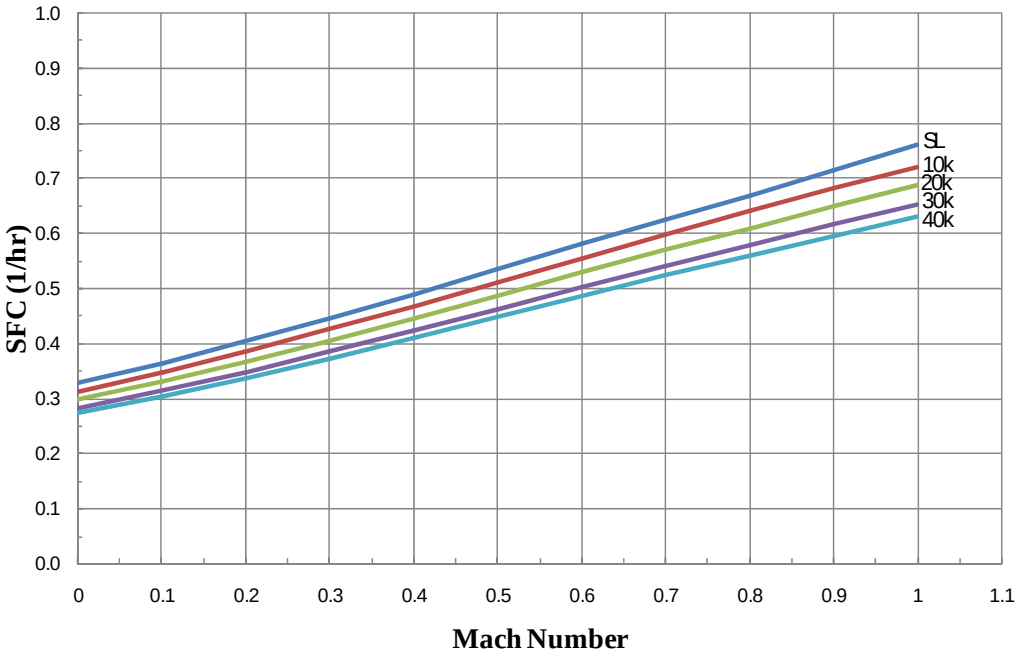

Figure 5.2: SFC versus Mach Number at Maximum Continuous Power

The F117's unique thrust reversing system is one of the main reasons for its selection. The engine has a core cascade thrust reverser in addition to the bypass cascade reverser, as can be seen in Figure 5.3. The cascade vanes direct the flow forward and upward. By reversing the entire engine flow, the engines are capable of providing reverse thrust even when the aircraft is standing still. Through a simple statics calculation, it is estimated that the engines are capable of backing the aircraft up a 4 degree slope. Directing the air upward has two advantages. First, the engines generate significant downward force on the wheels improving braking. Second, the engines do not blast the ground surface with exhaust gases effectively eliminating the hazard of debris ingestion. In addition, pilot visibility is not compromised on wet or dusty runways.

Figure 5.3: F117-PW-100 Bypass and Core Cascade Thrust Reversers (Ref. 12)

5.4 ENGINE NACELLE

The nacelles are extended well forward of the wing and supported by cantilevered pylons. The engine is placed well forward of the wing for many reasons. One, the engines receive relatively undisturbed air and smaller upwash angles. Two, the forward position allows the exhaust gases from reverse thrust to escape without impingement on the lower wing surface. Third, positioning the fan exhaust plane ahead of the wing provides great improvement in the maximum lift coefficient due to a favorable interference phenomenon (Ref. 15). Finally, the forward, under wing location of the nacelle allows for easy maintenance access. Table 5.3 shows the weight and dimensions of each nacelle that were determined by methods described in *Aircraft Design: Synthesis & Analysis* (Ref. 14).

Table 5.3: Nacelle Sizing

Nacelle	Value
Max. diameter (ft)	7.75
Length from inlet to engine exhaust nozzle(ft)	16.16
Total weight: engine nacelle, pylon, fuel system, oil system, etc (lb)	11360

6 WEIGHTS AND BALANCE

6.1 WEIGHT ESTIMATION

Keeping weight as low as possible has been a key concern throughout the design process. Airplanes are "bought by the pound" and the lower these weights are the lower to cost to the taxpayer. This philosophy drove many key design decisions on the YC-154 Skymaster II. A strut-braced wing was utilized to allow for much lighter wing structure to be used. This technology, normally reserved for small general aviation type aircraft, has been heavily studied at the Virginia Tech Department of Aerospace Engineering for use on larger aircraft. A twin-engine configuration was chosen over a four-engine design because of the weight savings brought on by physically not having two extra engines as well as the benefit of reducing drag, which in turn allows the design to be more efficient.

Two Class II statistical methods were utilized to estimate weight; the Torenbeeck Method and the General Dynamics Method. Both of these methods are laid out in Jan Roskam's *Aircraft Design: Series* (Ref 4). The two methods rely heavily on statistical data gathered from historical aircraft of similar classes. The Skymaster II is considered to be a Military Transport aircraft and is classified as such by both methods.

The key assumptions that were made were on adjustments to the weights calculated by each method to account for use of the weight saving technologies that are around today. Most of these assumptions were made in the structural weight calculations.

Table 6.1: Structural Component Weight Adjustment Assumptions

Component	Assumptions
Wing	-19% for strut bracing, -5% for two engines under-wing -5% Fuselage Mounted LG, +7% for High Lift system
Empennage	-15% for use of composite empennage
Landing Gear	+10% for soft field TO and Landing

Most of the assumptions came directly from the Roskam (Ref 4) method; the only assumptions that were not used from this reference were the 19% reduction in wing weight from the strut and the 10% increase of weight from the landing gear. The 19% wing weight reduction assumption came from Gundlack (Ref 15), which studied the effects on wing weight with and without a strut. Even with the decrease the standard "rule of thumb" of 8 pounds per square foot of wing area gives a good check to prove that the wing weight is achievable. The 10% increase comes from the analysis of the landing gear done to ensure that the aircraft can land on a California Bearing Ratio 4-6 surface.

6.1.1 Structural Weight Breakdown

Table 6.2: Structural Component Weight Breakdown in Pounds

	Pre-Adjusted				Adjusted			
Structural Weight	**GD**	**Torenbeeck**	**Average**	**Wi / TOGW**	**GD**	**Torenbeeck**	**Average**	**Wi / TOGW**
Wing Weight	15394.3	22347.0	18870.6	0.097	12007.5	17430.6	14719.1	0.075
Horizontal Tail	1064.3	1086.6	1075.5		904.7	923.6	914.1	
Vertical Tail	1346.7	1392.9	1369.8		1144.7	1184.0	1164.3	
Empennage	2411.0	2479.5	2445.3	0.013	2049.4	2107.6	2078.5	0.011
Fuselage	10778.9	6800.3	8789.6	0.045	9485.5	5984.3	7734.9	0.040
Landing Gear	5217.8	5217.8	5217.8	0.027	5739.6	5739.6	5739.6	0.029
Total	**33802.1**	**36844.6**	**35323.4**	**0.181**	**29282.0**	**31262.1**	**30272.1**	**0.155**

The structural weight break down takes advantage of the two different methods by using them to check each other and provide an average weight total. This eliminates any point errors that may have occurred during the compilation of the historical data. As can be seen in Table 6.2 the two methods are within 7.4% of each other in total structural weight. The weight fractions also compare nicely to those of C-141 and C-130 which are aircraft on the top and bottom end of the weight spectrum for the aircraft.

6.1.2 Fixed Equipment Weight Breakdown

Table 6.3: Fixed Equipment Weight Breakdown in Pounds

System	Weight (lbs)
Flight Control System	3924.7
Hydraulic System	1852.5
Electrical System	5021.1
Avionics/Instrumentation	4793.3
Pressurization,A/C,Deicing	3800
APU	2535
Furnishings	3000
Paint	1170
Fixed Equipment Weights (lbs)	**26096.6**

The fixed equipment weight can be seen in Table 6.3 and shows what allotments were made for each system onboard the aircraft. These allotments are taken from historical data that has been compiled and used as a guide in both the Torenbeeck and General Dynamics methods of weight estimation. At 26,100 pounds the fixed equipment weight fraction (W_{FE}/TOGW) is 14% of the total aircraft weight. No adjustments were made to these calculations for the sake of conservatism. Some of these weights seem high, specifically Avionics and Instrumentation and the APU weight. Typically aircraft will use as much fixed equipment as is allotted in the design and this will allow the aircraft to have expandability in the future.

6.1.3 Total Weight

For the combat mission the total weight of the aircraft is 182,000 lbs. This includes a weight estimate of 11360 lbs for the engine, nacelle, pylon, fuel system, oil system, and starting system. These weights were estimated as part of the propulsion analysis. By taking advantage of composite materials, using a strut-braced wing, using a twin engine configuration, and tailoring the mission profile every conceivable effort was made to reduce weight. At 182,000 pounds, the C-154 Skymaster II falls between the C-17 and the C-130 on the weight spectrum.

6.2 BALANCE

Table 6.4: Aircraft CG Location For Combat Mission

Component	Weight	x location	% of Fuselage Length	y location
Fuselage	7734.89	62.92	0.44	8.67
Wing	14719.08	59.44	0.42	16.49
Horizontal Tail	914.14	148.72	1.04	35.50
Vertical Tail	1164.34	140.14	0.98	20.40
Main Gear	4878.66	68.64	0.48	1.36
Nose Gear	860.94	25.21	0.18	1.53
Flight Control System	3924.66	85.80	0.60	7.82
Hydraulic System	1852.50	75.79	0.53	17.00
Electrical System	5021.12	62.92	0.44	5.95
Avionics/Instrumentation	4793.32	10.01	0.07	0.85
Pressurization,A/C,Deicing	3800.00	84.37	0.59	1.36
APU	2535.00	140.14	0.98	16.30
Furnishings	3000.00	81.51	0.57	7.31
Paint	1170.00	78.65	0.55	7.14
Powerplant Weight	23086.00	60.06	0.42	7.31
****Estimate From Prop Group**				
Mission Fuel	46000.00	61.20	0.43	16.49
Crew	600.00	20.02	0.14	11.00
Payload	60000.00	66.50	0.47	8.67
Mission Segment	**Horizontal CG Loc**	**% Fuselage Length**	**Vertical CG Loc**	**% Fuselage Height**
First Takeoff	64.90	0.45	10.99	0.65
First Landing	65.09	0.46	9.90	0.58
Second Takeoff	64.78	0.45	10.71	0.63
Second Landing	64.79	0.45	9.10	0.54

Table 6.4 shows the combat mission CG location as calculated using Roskams (Ref 4) method. The location and weight of each component was determined and then using equation 6.1. The horizontal change of the CG is from 24.40% MAC to 25.50% MAC.

$$\bar{x} = \frac{\sum_{1}^{i} m_i x_i}{\sum_{1}^{i} m_i} \qquad \text{Eq. 6.1}$$

The vertical CG was calculated in much the same way, only using the y-location instead of the x-location. The vertical CG was important in determining stability both in flight and on the ground.

With a transport aircraft the major concern is CG shift as payload is on and off loaded. Figure 6.2 shows the CG travel of the aircraft in both the horizontal and vertical directions. This will be mitigated by providing loading procedures through a dedicated Field Manual to allow ground crews to safely position cargo to allow minimum CG shift through the mission.

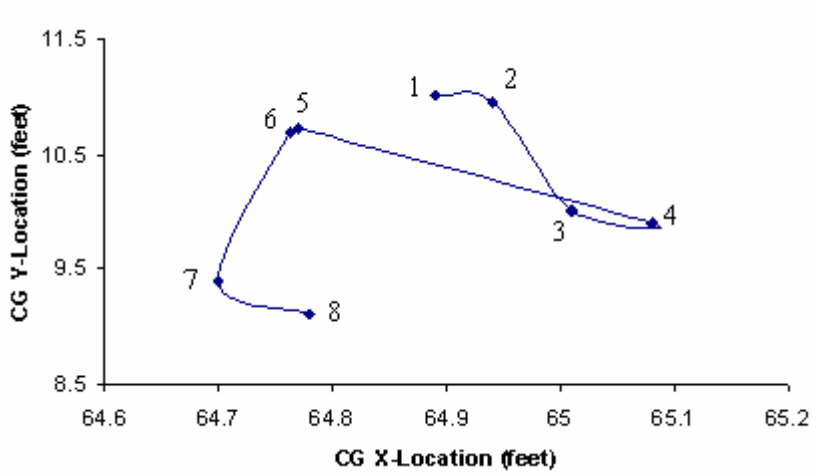

Figure 6.1: CG Travel

7 STABILITY AND CONTROL

7.1 DESIGN PHILOSOPHY

A Fly-by-wire control system will be used on the Skymaster II, because of its weight savings and survivability. All sizing was compared to historical data of other STOL aircraft,

namely the C-17 Globemaster III, and is a traditional configuration. Control surface deflections for all flight conditions, engine out and crosswind analysis, dynamic stability, and being able to trim at C_{Lmax} were all major drivers in the layout of the Skymaster II. With a relatively low static margin for military T-tail transports, the Skymaster II was able to perform all tasks set by the RFP and FARs.

7.2 TAIL DESIGN

Tail size and type are integral parts of an aircraft in that the tail provides the majority of the aircraft's stability. Boom tail, T-tail, and conventional tail designs were all considered for our transport concept. Each tail style has its benefits and drawbacks, which we carefully analyzed.

The T-tail design was chosen because of its ability to move the horizontal tail out of the wing high-lift system wake, its weight savings due to a smaller required tail area, and the increased moment arm gained from extending the horizontal stabilizer aft of the fuselage. An increase in leading edge sweep, as compared to the wing, was used for the horizontal tail to allow for a higher critical mach number on the horizontal tail, ensuring that the wing stalls before the tail. Tail sizes were initially estimated using Raymer (Ref 2) method and finalized based on wing location, static margin, and other stability characteristics. Table 7.1 gives the geometric sizing of the Skymaster II's horizontal and vertical tails.

Table 7.1: Tail Geometry Data

	Horizontal Tail	Vertical Tail
Span (ft)	44	18.5
Sweep (deg.)	20	38
Area (ft^2)	352	259
Taper Ratio	0.32	.75
Volume Coef.	1.07	0.07

7.3 CONTROL SURFACES

Initial sizing of the control surfaces was based off historical data and comparisons to other similar STOL aircraft. Sizing was altered to its final state after analysis of the control derivatives was completed. The ailerons will consist of the outer 20 feet of each wing consisting of a chord length of 25% of the wing chord. Ailerons of this size will be needed to counter act the large roll moments created by powered lift with an inoperable engine.

The elevator, with a chord length of 35% of the horizontal tail chord, will be double hinged extending on the outer 90% of the horizontal tail. The rudder will be double knuckled, to allow for greater surface deflection and more effectiveness, consisting of 85% of the vertical tail span with a chord length equal to 30% of the vertical tail chord. Figures 7.1 and 7.2 show two-dimensional views of the horizontal and vertical tails with the stabilizers shaded.

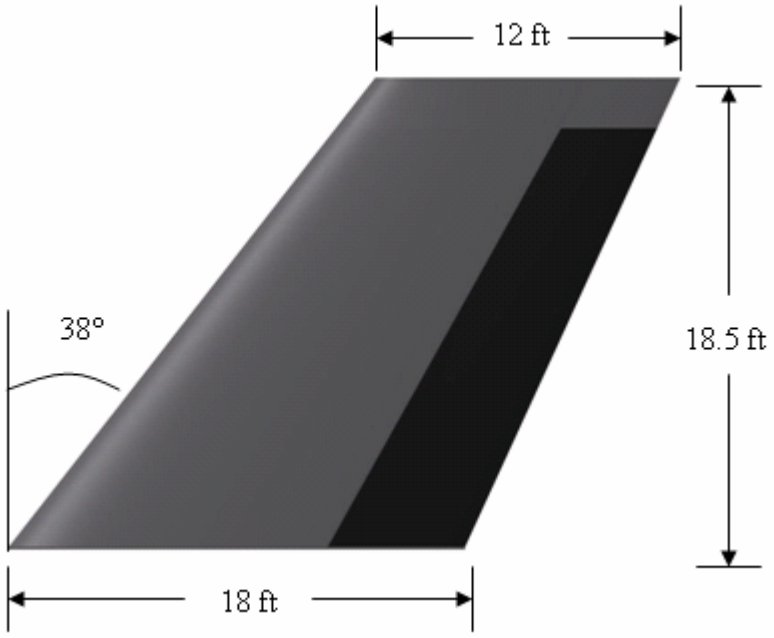

Figure 7.1: Vertical Stabilizer

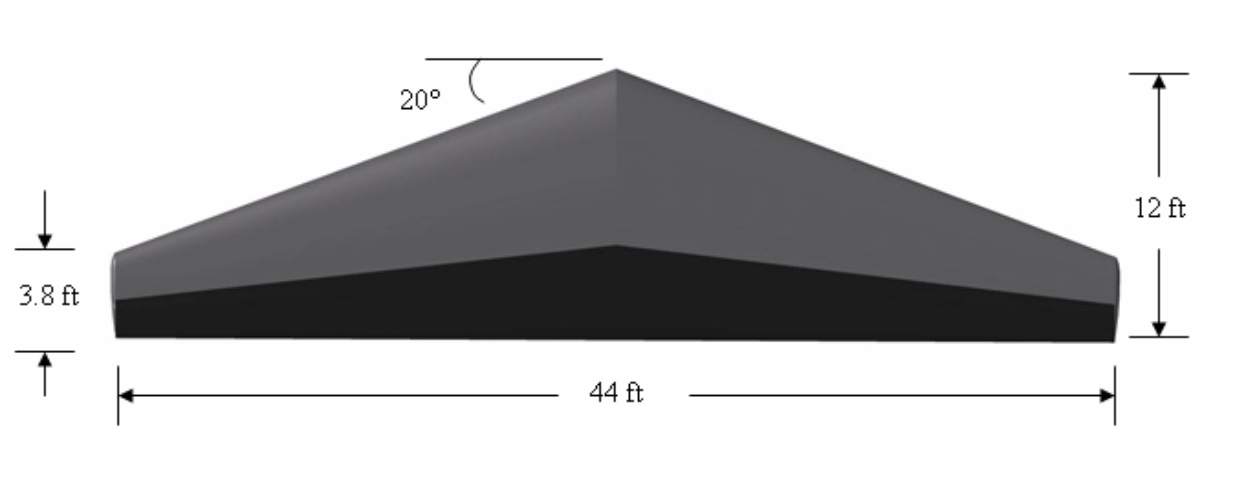

Figure 7.2: Horizontal Stabilizer

7.4 Stability and Control Derivatives

The program *JKayVLM*, written by Jacob Kay at Virginia Tech (Ref 21), was used to find stability and control derivatives using the Vortex Lattice method. The lateral and longitudinal geometry of the aircraft were approximated by using trapezoidal shapes. Stability and control derivatives were calculated at the takeoff, cruise, and landing flight phases. Details of each flight condition and the derivatives for all three flight conditions can be found in Tables 7.2 and 7.3 respectively.

Table 7.2: Flight Conditions

Flight Phase	Takeoff	Cruise	Landing
Altitude(ft)	50	30,000	50
Speed(knots)	116.7	529.2	130.3
CG location (%MAC)	23.40%	24.90%	25.50%

Table 7.3: Stability and Control Derivatives

Flight Phase	Cruise	Takeoff	Landing
$C_{L\alpha}$	8.412	5.872	5.89276
$C_{m\alpha}$	-1.438	-0.7607	-0.63673
C_m/C_L	-0.171	-0.12954	-0.10805
C_{Lq}	20.694	16.20142	15.95981
C_{mq}	-64.29	-52.8472	-52.59638
$Cl_{\delta e}$	0.3006	0.25035	0.2509
$C_{m\delta e}$	-1.753	-1.43223	-1.43031
$C_{l\delta a}$	-0.808	-0.57345	-0.57553
$C_{n\delta a}$	-0.005	-0.00381	-0.00382
$C_{Y\delta r}$	-0.158	-0.17934	-0.17928
$C_{l\delta r}$	-0.019	0.02131	0.02131
$C_{n\delta r}$	0.0837	-0.09419	-0.09377
$C_{Y\beta}$	-0.516	-0.47479	-0.47528
$C_{n\beta}$	0.1857	0.16663	0.16583
$C_{l\beta}$	-0.06	-0.04951	-0.0496
C_{Yr}	0.5342	0.49158	0.49004
C_{nr}	-0.254	-0.23348	-0.23195
C_{lr}	0.0548	0.04993	0.04979
C_{lp}	-0.783	-0.56246	-0.56446
C_{np}	-0.412	-0.34342	-0.34447

7.5 LATERAL AND LONGITUDINAL DYNAMICS

Ensuring the handling qualities of the Skymaster II was completed using *CPRCheck* and Roskam's (Ref 4) methods. The stability and control derivatives listed in Table 7.3 were used. Level 1 class A, B, and C flight categories were considered. Tables 7.4 and 7.5 list the data for short period, phugoid, and Dutch roll modes, along with data for time to bank and roll mode time constant. All of the Skymaster II handling qualities are also compared in Tables 7.4 and 7.5 with the Level 1 Military specifications listed in MIL-F-8785C. Skymaster II is within the Level 1 requirement for all the tested conditions.

Table 7.4: Class A and C Dynamics

Class A and C Flight Categories	MIL-F-8785C		Takeoff	Landing
	Minimum	Maximum		
ω_{SP}	0.28	3.6	0.80	0.83
ζ_{SP}	0.35	1.3	0.75	0.80
ζ_{Ph}	0.04	--	0.10	0.07
ζ_{DR}	0.19	--	0.20	0.21
ω_{DR}	0.4	--	0.52	0.70
t_{30deg}	--	1.4	1.08	1.25
τ_r	--	1.4	0.13	0.16

Table 7.5: Class B Dynamics

Class B Flight Category	MIL-F-8785C		Cruise
	Minimum	Maximum	
ω_{SP}	0.3	2	1.72
ζ_{SP}	0.085	3.6	0.59
ζ_{Ph}	0.04	--	0.06
ζ_{DR}	0.08	--	0.12
ω_{DR}	1	--	1.81
t_{30deg}	--	1.4	0.32
τ_r	--	1.9	0.27

7.6 Engine Out and Crosswind

The RFP requires the Skymaster II to be capable of taking off with one engine inoperative. Engine out requirements were calculated using *LDstab*, written by Joel Grassmeyer from Virginia Tech (Ref 22). Engine out is most critical in the takeoff configuration due to the slow speed. Aileron and rudder deflections necessary to takeoff with engine out are listed in Table 7.6. The rudder is kept at maximum deflection and the bank angle is set to the maximum of 5 degrees.

Austere landing zones in combat often cause the runway to be oriented in a less than optimum position. Due to this the RFP states that the Skymaster II must be capable of landing with a 25 knot crosswind along with a 5 knot tailwind component. Data for landing in a

crosswind is included in Table 7.6. Aileron and Rudder deflections are both within the maximum deflections of 25 degrees.

Table 7.6: Engine-out and Crosswind Landing Deflections

Landing Situation	Engine Out	Crosswind
Bank Angle(Φ)	5°	1°
Rudder Deflection(δ_r)	25.00°	21.03°
Aileron Deflection(δ_a)	15.04°	21.62°

Single engine minimum control speed was also calculated and checked with the stall speed of the aircraft. Figure 7.3 shows that at all times our minimum control speed is lower than our stall speed which is ideal. The minimum control speed plot is broken into two branches. The left branch is with the rudder deflection held at its maximum with aileron deflection varying while the right branch has constant maximum aileron deflection with varying rudder.

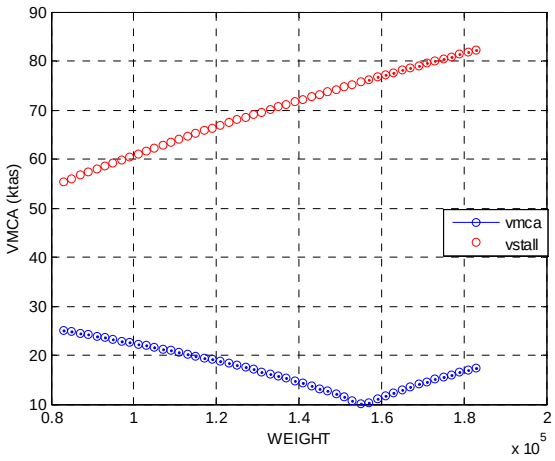

Figure 7.3: Single Engine Minimum Control Velocity

7.7 TRIM AT C_{LMAX}

The Skymaster II uses externally blown flaps to create the lift necessary to takeoff and land in STOL conditions. Using Roskam (Ref 4) methods elevator deflections were calculated at different lift coefficients verifying that the Skymaster II can be trimmed to its maximum

attainable C_{Lmax} of 4.2. The necessary elevator deflection needed to trim at C_{Lmax} was found to be -23.21°, which is well within the maximum deflection of -30.00°.

8 STRUCTURES

8.1 DRIVERS

The aspects of this design that have the biggest impact on the structural design of this aircraft are the speed and payload requirements. This aircraft is required to achieve an eight tenths Mach cruise speed, which will put a demand on the wing to have a large aspect ratio, and a small cross sectional profile to reduce drag. The short takeoff and landing requirement places a high lifting load on the wing to get off the ground in the required distance. Both of these stipulations will require this plane to be as light as possible, and as aerodynamically efficient as possible. The structural design and materials selection of the aircraft are critical to both of these goals, which is perhaps less obvious for the latter than for the former.

8.2 V-N DIAGRAM

The first step in any structural design is to know what range of loads the aircraft is expected to perform under. This is done by knowing the weight of the aircraft, and the load factors that are being applied in maneuvering. The V-n diagram in Figure 8.1 was produced using a Matlab code written by Patrick LeGresley of Stanford (Ref 16). It uses basic inputs about the aircraft's geometry and flying conditions to calculate and plot load factors against velocity.

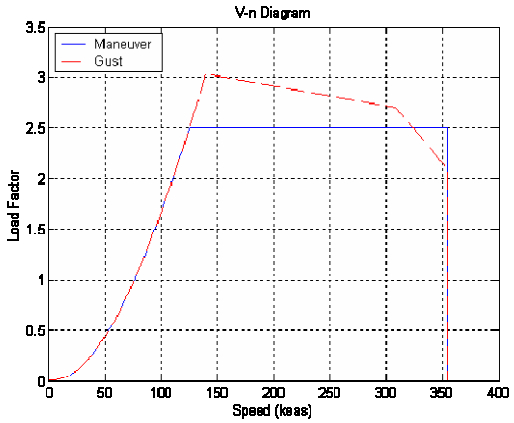

Figure 8.1: V-n Diagram

From the information on the plot, the structure of this aircraft should be designed to sustain loads that are three times the weight of the aircraft itself. Since this is a transport aircraft, it is not being designed to perform high load maneuvers, nor is it expected to perform at negative load maneuvers. A negative loading factor of one will be used to account for the unexpected, and for bouncing on the tarmac.

The structure of this aircraft is designed to minimize weight and maximize the effectiveness of the wing. As with most aircraft, weight is a major consideration, but for this aircraft it is even more important. The short takeoff and landing requirement makes getting off the ground a more complex analysis. Every pound that can be shed here will make it easier to takeoff in the twenty five hundred feet allowed. Saving structural weight in the beginning improves weight twofold. Not only is the structure lighter, but less fuel needs to be carried to haul that weight around. Then the wings don't have as much to lift, and can be made smaller, which is less drag, and more fuel savings. It is obvious that keeping the structural weight down was important, especially since we're already lifting thirty tons of vehicle and supplies.

8.3 STRUT

The most immediate answer to help with the structural weight is to use a strut-braced wing. In *Multidisciplinary Design Optimization of a Strut-Braced Wing Transonic Transport* (Ref 15) it is stated that using a strut-braced wing can save as much as 16% of structural and fuel weight. Loads specific to this aircraft were analyzed to be sure that a strut-braced wing would work for it. Unfortunately the forces on a strut-braced wing and its strut are statically indeterminate, making the analysis much more difficult. A program was written using a work-energy method and Castigliano's Theorems to calculate the internal forces generated by the loads on the wing. This program also recommended certain wing box and strut dimensions. Figure 8.2 is a plot of the moment forces acting along the wing span of the strut-braced wing. The discontinuities in the following two plots are due to the engines.

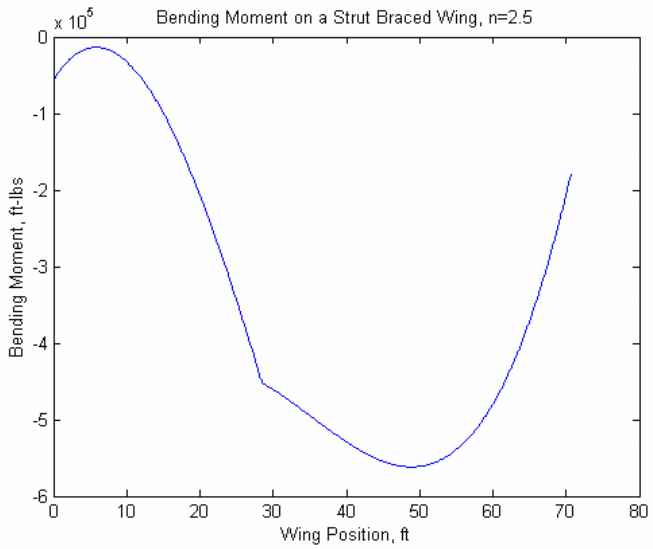

Figure 8.2: Bending Moment Acting on Strut-Braced Wing

It was found that the best position for the strut to attach to the wing was as far out as possible, so it has been placed on the wingtip. This position has the added benefit of acting as a winglet, making use of the strut even more advantageous. Notice that the bending moments are all negative, as opposed to positive, as they usually are. This is because the strut holds the tip

stationary. As aerodynamic lift pulls up, it tends to bow up the wing, creating the negative moments.

To compare the forces to those experienced by a standard cantilevered wing, a similar analysis was preformed. Figure 8.3 depicts the moments seen by a cantilevered wing. However, the structure could not be made thick enough given the dimensions of the wing to withstand the stresses produced, which are an entire order of magnitude larger than the strut-braced wing. To be able to make a realistic comparison, the cantilevered wing had to be doubled in thickness. The structure also had be made thicker, and in the end required 37.5% more material in just the wing box as compared to the strut-braced wing to hold up to the same loads.

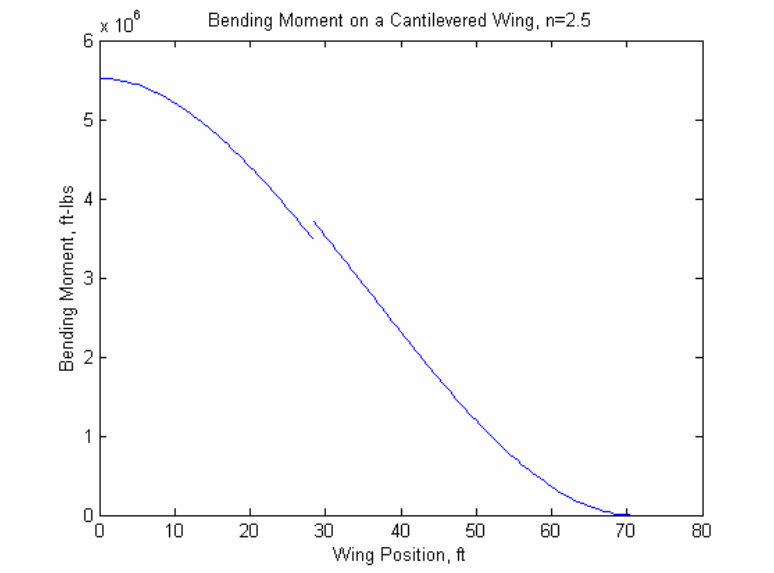

Figure 8.3: Bending Moment on a Cantilevered Wing

Another benefit of the strut-braced wing is that a larger aspect ratio wing can be used more effectively. This is immensely helpful in reducing drag at transonic speeds. Also, since the strut is holding the wingtip down and it is not being allowed to bend up, the wing stays flatter, which makes it more efficient at producing aerodynamic lift. All of these factors together made a strut-braced wing an easy choice.

8.3.1 Strut Design

A perhaps unobvious documented problem with struts at trans-sonic speeds is the tendency to develop a strong shock where the strut meets the wing. This problem was studied extensively in *Transonic Aerodynamics*, by Ko and Mason (Ref 17). It was discovered that the cause of the shock was a nozzle effect being caused by the foil shape of the strut and its proximity to the wing. The nozzle was formed by the cross sectional gap between the wing and the strut. This problem was also easily remedied by two methods. The first is to increase the pylon length so that the ratio of the "inlet" area to the "throat" area is less than the "choked" *A/A** value of 1.0382 for eight tenths Mach number speeds. Secondly, by flattening the top side of the strut foil the change in area going through the 'nozzle' is reduced, thereby reducing the wave drag. Incorporating both of these solutions into this design, the strut is attached to the wing via a vertical pylon, and the strut foil shape will be modified to flatten on the top as it approaches the pylon. Since the strut is being attached to the wingtip in this case, the pylon will also act as a winglet.

8.4 Negative Loading

This aircraft is not expected to encounter high negative loading stresses, so the structure is designed with a maximum negative load factor of one. The biggest problem with negative loading in this aircraft lies with the strut. The strut is designed to operate with high tensile loads, and an idealized long slender rod works well for this purpose because it is allowed to stretch. In compressive forces, however, this idealized rod is begging to buckle. To overcome this problem a telescoping strut system is being utilized to ensure that the structure of the strut doesn't encounter negative loading. The strut is modeled as a wire "rope", which works in tension only. This rope is then shrouded in an airfoil so as to reduce the aerodynamic costs of the extra

appendage. The strut attaches to the fuselage at the same point as the landing gear, which provides extra space for the telescoping mechanism, and consolidates two key structural junctions. Where the strut runs into the fuselage a hydraulic piston takes in the slack on the rope as the strut compresses, as in Figure 8.4. As the load on the wing increases, the strut telescopes out until it is fully engaged, as shown in Figure 8.5. At the same time the airfoil shroud is allowed to telescope in and out as required, and doesn't bear any load. As the loads become positive, the strut telescopes out, and the rope begins taking on tensile loads.

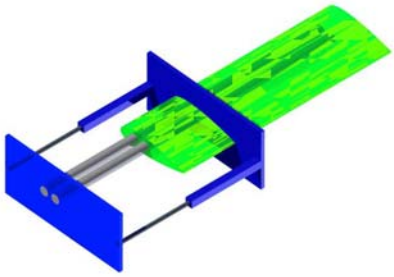

Figure 8.4: Retracted Strut

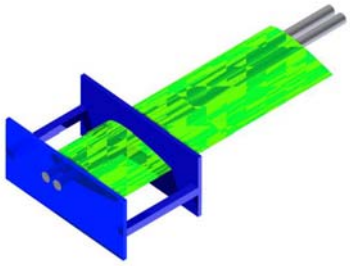

Figure 8.4: Engaged Strut

8.5 MATERIALS

Initially this aircraft was to be made of all time proven materials – mostly aluminum and steel. Composites were viewed as too unreliable in damage control situations, as well as too costly. Since this transport will be subjected to hostile landing areas, survivability needs to be considered. Composites seem to have a reputation of shattering when struck, as with a dropped wrench, or a bullet. An airplane with a composite wing that is shot could shatter, and the aircraft might not make it back. Even if it did make it back it would be out of commission until the wing could be replaced. Whereas an aluminum wing would just have a bullet sized hole in it, and it could be patched up easily enough. Today, however, composites are continuing their march forward, and are no longer the fragile, irreparable materials of the past. Now a composite skin can self-heal fatigue cracks and larger holes can be repaired in the field using a laser. Composite materials are a fraction of the weight of their metal counterparts, and are stronger by weight, especially since their fibers can be oriented to maximize their effectiveness. On the downside, composites are still expensive, although new processes are always bringing the costs down. As mentioned earlier, saving structural weight also saves fuel weight, and operating costs. Although the initial costs of using composite materials may be more expensive compared to the traditional materials, the saved fuel costs over the life of the aircraft will more than offset that initial expense, especially with the rising cost of fuel. With that in mind a goal was set of using 20% composite materials in this aircraft. That goal can be reached by using composite materials for items such as the engine nacelles, internal fuselage components, and parts of the skin. Still, the wing box will be made of aluminum, and the strut core will be steel. This is because of the importance for these parts to be able to plastically deform. The strut can not be allowed to completely fail, because if that happens, the wing becomes a cantilevered spar and will surely

diverge under such loading. Incidentally, the steel wire rope core being used for the strut will have a redundant backup to prevent exactly this problem.

Table 8.1: Materials Selection

Material	Density [lbs/in^3]	Tensile Strength [ksi]	Modulus of Elasticity [ksi]
AS/3501 Carbon/Epoxy	0.058	1447	138
Kevlar 149/Epoxy	0.05	1280	87
PM-15 Carbon/FyreRoc	0.06	25	5500
Alclad Aluminum 2014-T6, T651	0.101	60	10500
17-7 PH Stainless Steel, CH900, wire	0.282	365	29600

The relevant properties of the materials chosen are summarized in Table 8.1. Stainless Steel was chosen for the load bearing portion of the strut for its extremely high modulus of elasticity and tensile strength. It's also very heavy, but this is a necessary tradeoff. It is necessary for the strut to be able to elastically deform without yielding to endure the high tensile loads that will be placed upon it. For the main structure an aluminum alloy was chosen. This aluminum isn't as strong as the steel, but it's half as heavy. It provides sufficient strength, while saving structural weight. For the skin of the wings and tail, a carbon fiber reinforced in an epoxy resin matrix was found to be best suited. Its weight is half that of traditional aluminum and it packs more than enough strength to stand up to the wing loading. The material switches to a Kevlar and epoxy composite at the fuselage because it's a bit lighter, but provides comparable strength. Externally blown flaps have created a unique problem in materials selection because of the high temperatures of the engine exhaust being directed to the flaps. Titanium alloys have been used more traditionally for this purpose. However, a proprietary composite utilizing carbon fibers in a resin matrix called FyreRoc has been shown to withstand temperatures up to 2000 °F without any permanent deformation, smoking, or release of toxic fumes. Perhaps more importantly, this

material maintains its strength properties at these temperatures, and it's about as dense as the other composites selected, so it too saves structural weight.

9 LANDING GEAR

9.1 GEAR SIZING AND SELECTION

The Skymaster II is required to land on surfaces with a CBR range of 4.0 to 6.0 which is equivalent to packed sand or clay with a poor foundation. Due to this unimproved soft surface the tire pressure is set at 50 psi. The need for low tire pressure significantly reduces the load carrying ability of the gear but increases contact area. Figure 9.1 studies the tradeoff between the number of main gear wheels needed to support the aircraft's weight versus their size.

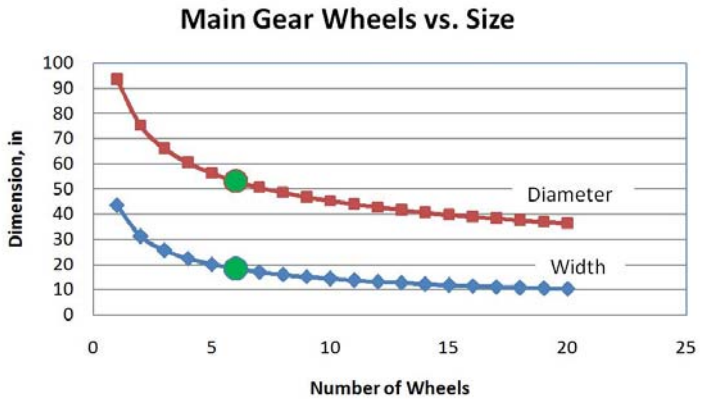

Figure 9.1: Main Gear Tire Size vs # of Wheels

The curves show for the Skymaster II's weight the optimal number of wheels for the main gear is 6, where the curves begin to level out. The tires will need to be manufactured to specification for the aircraft because of the landing surface and aircraft weight. Table 9.1 lists the tire details for the nose and main gear. All tire and shock values were found using Raymer's (Ref 2) tire sizing method and historical data.

Table 9.1: Aircraft Wheel and Tire Information

	Nose Tire	Main Tire
Number of Wheels	2	6
Diameter	35 in	53 in
Width	10 in	18 in
Rim Diameter	13.5 in	20 in
Loaded Rolling Radius	14.1 in	18.7 in
Deflection	3.4 in	7.8 in
Pressure	50 psi	50 psi
Tube / Ply	TL / 25	TL / 30
% Aircraft Weight	8.15%	91.85%
Weight Per Tire	7420 lb	27860 lb

The weight per tire is the actual load the tire will experience, however the specs for the tire allow a factor of safety and a safe landing if one of the main tires were to malfunction and/or be damaged. This is a military aircraft and high vertical velocities can be expected when landing, up to 15 feet per second. The 6 main gear struts will need to absorb lots of energy on impact and will be hydraulic shock absorbers with ride height control for loading purposes. Table 9.2 contains the main gear strut details.

Table 9.2: Main Gear Hydraulic Shock Absorbers

Emergency Landing Weight	182000 lb
Vertical Velocity	15 ft/s
Vertical Kinetic Energy	635870 ft-lb/s
Gear Factor, N (Military Transport)	3.0
Load on Shock	91000 lb
Stroke at Landing	13.9 in
Tire Stroke	7.8 in
Length	34.7 in
Diameter	10.4 in
Piston Diameter	7.3 in

The stroke listed in the table is the actual stroke that the shock takes however there is a 1 inch factor of safety added to piston travel. The main gear strut also has a large drag/braking brace because of the large braking force exerted on it, as shown in Figure 9.2. Table 9.3 outlines the braking requirements of the main gear.

Table 9.3: Main Gear Braking

Emergency Landing Weight	182000 lb
Braking Kinetic Energy	5.32E7 ft-lb/s
Per Wheel	8.87E6 ft-lb/s
Recommended Rim Diameter	17 in
Braking Force	36869 lb
Per Wheel	6145 lb

All of the energy from braking is converted into heat. This requires that the rims to be large enough to support brakes with enough material to absorb the heat.

9.2 Gear Location and Arrangement

The main gear will be located in the belly of the Skymaster II just aft of the CG. The gear assembly will consist of 6 wheels in 2 rows with their own strut. The main gear doors will open in two parts and the gear will rotate 90 degrees down into landing position. The nose gear will consist of two wheels side by side with a single strut. Figure 9.2 shows the gear sequence.

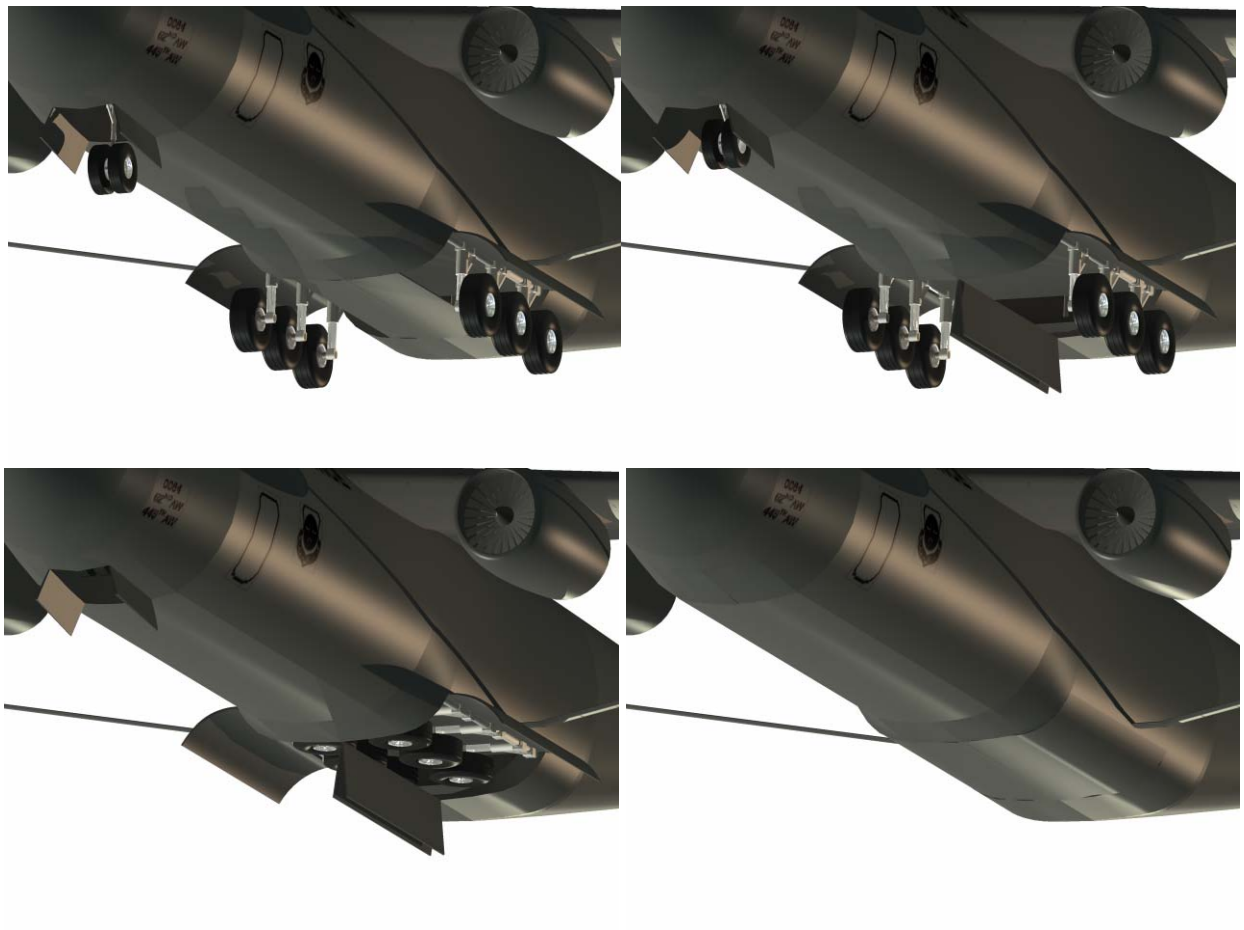

Figure 9.2: Main Gear Layout and Deployment

Since the gear deploys from the middle of the aircraft outward the tires provide a wider stance on the ground. This allows for a narrow fuselage without the use of pods to obtain ground stability, which reduces drag.

Roskam states that the side-to-side stability angle cannot exceed 55 degrees and this is the difficult angle to meet. The front to back stability angle cannot fall below 15 degrees as noted in Figure 9.3 below. Both angles are measured within relation to the gear through the CG of the aircraft.

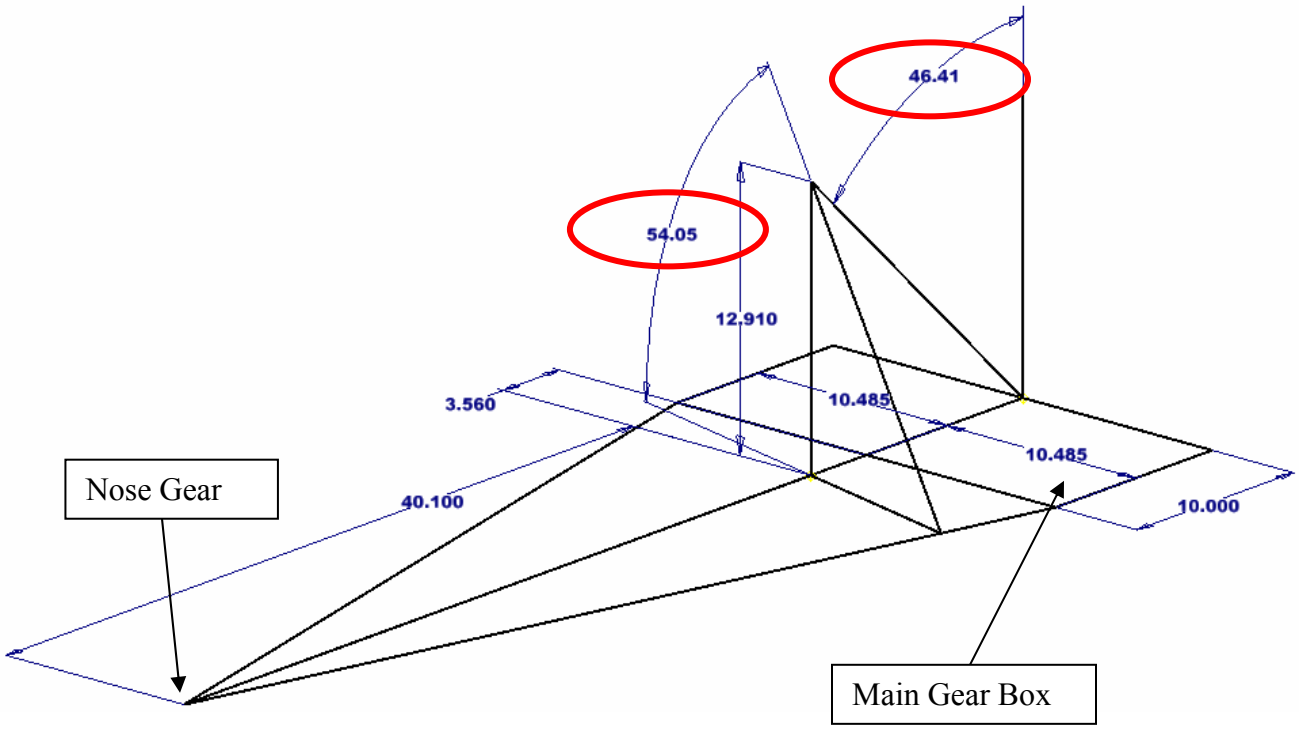

Figure 9.3: Landing Gear Stability Diagram

10 SYSTEMS

Although most aircraft systems and subsystems do not have a major impact on the initial design layout, these systems must be accommodated for at some point in the design cycle. Therefore, it is appropriate to briefly review some of the critical airplane systems driving the design of our military transport.

10.1 AVIONICS

Based on the typical avionics weight fractions as well as the avionics density outlined in Raymer (Ref 2), this design will require roughly 2,000 lbs or 50 ft^3 of avionics. To reduce the cost and complexity associated with multiple avionics suppliers, the design will utilize an integrated avionics suite offered by Rockwell Collin Inc. This package will include a communications and information management system, a flight control system, a flight displays

system, a hazard detection and traffic management system, an engine indicating and crew alerting system as well as a navigation and landing system.

Figure 10.1: Flight Deck Layout (Rockwell Collins)

10.2 FUEL SYSTEM

The fuel system is comprised of fuel tanks, fuel pumps, fuel lines, vents and control valves. In general, fuel tanks are the only component of the fuel system that affects the aircraft layout. According to the mission performance analysis, a transport category aircraft with a takeoff gross weight of 182,000 lbs will require roughly 70,000 lbs of fuel for the ferry mission. Assuming JP-8 with a Mil-spec density of 6.7 lb/gal, this translates to a fuel tank capacity of roughly 10,500 gal and a volume of 1,400 ft^3. A conventional configuration of two main wing tanks and a center tank is preferable since it optimizes the use of space in the wing box and reduces wing bending moment. Auxiliary fuel cells may be installed in the dry bay for extended range operations.

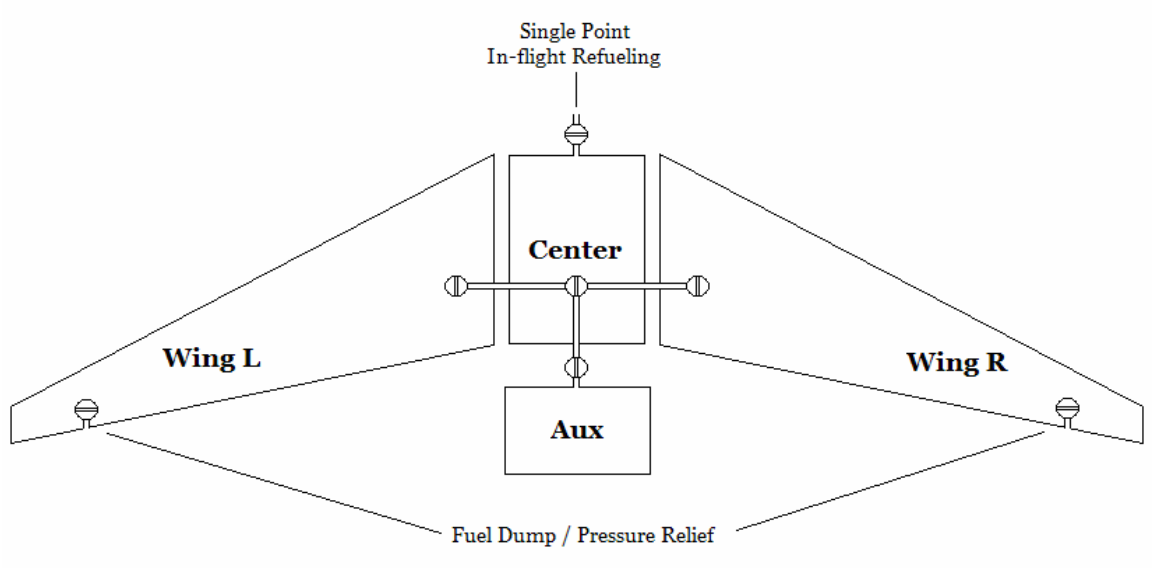

Figure 10.2: Fuel System Layout

Fuel tanks are divided into three main categories; discrete, bladder and integral. Discrete tanks are fabricated separately and installed on the aircraft. This type of tank is used on many light general aviation aircraft. The auxiliary fuel cells will be a combination of removable discrete tanks. Bladder tanks are essentially thick rubber bags placed in the structure of the aircraft. A bladder tank has the advantage of being self-sealing which increases aircraft survivability in a combat environment by preventing leaks caused by bullet penetration. According to Raymer, a bladder tank causes a loss of approximately 10% in available volume. Despite their benefits, bladder tanks will not be used on our aircraft since wing volume is already limited by wing thickness. Integral tanks are the simplest type of tank and are created by sealing cavities in the existing structure. This is the preferred tank type for the wing and center tanks. A porous foam material is usually added to an integral tank to reduce fire hazards associated with structural damage. Raymer states that a 2.5% increase in unusable fuel is associated with this material since it tends to absorb fuel. A 3-5% increase in fuel volume will be accounted for due to temperature variations. An in-flight refueling receptacle situated on the upper fuselage will be

incorporated into the fuel system design to allow for refueling from a boom style tanker. Fuel jettison capability will provided by valves located near the wing trailing edge.

An Onboard Inert Gas Generating System (OBIGGS) is critical to our design. The system will use nitrogen enriched bleed air from the engines to inert fuel vapors in the main and auxiliary fuel tanks. The system is designed to prevent an explosion of fuel vapors in the event that the structural integrity of a fuel tank is compromised. The OBIGGS system will also pressurize the fuel tanks to supply fuel to the engines and the auxiliary power unit. Electric fuel pumps will supplement fuel transfer between main and auxiliary fuel tanks. At the heart of the OBIGGS system is a lightweight aluminum pressure vessel containing a polymer fiber separator membrane depicted in the figure below.

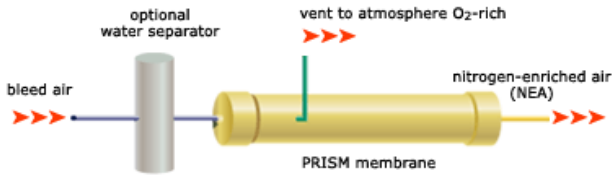

Figure 10.3: OBIGGS System (Air Products & Chemicals Inc)

Weight is dependent on the level of performance required; each separator varies between 5 lbs and 20 lbs. A rough weight estimate of the OBIGGS system to be installed on this aircraft is 1,500 lbs.

10.3 Flight Control System

Central hydraulic systems add weight and complexity to the aircraft structure. These systems must generate and maintain between 3,000 lb/in^2 and 6,000 lb/in^2 in each hydraulic circuit at all times. A single hydraulic circuit is often used by multiple actuators for flight control, flaps, spoilers, speed brakes and landing gear. A fault in any hydraulic line often renders

the entire circuit useless. Therefore, additional circuits are installed to ensure system redundancy. Removing this system decreases the personnel and support equipment required to maintain the aircraft. Furthermore, efficiency and reliability can be increased through the use of electro-hydrostatic and electromechanical actuators in place of a centralized hydraulic system. Electro-hydrostatic actuators utilize an electric motor to pump self-contained hydraulic fluid to a piston. Electromechanical actuators use a gearbox in place of internal hydraulic fluid. The figures below depict both electro-hydrostatic and electromechanical actuation systems.

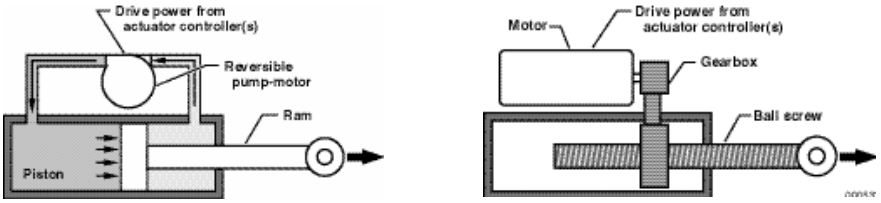

Figure 10.4: Electro Hydrostatic and Electro Mechanical Actuators (NASA)

If an actuator fails, the individual component may be isolated by switching the control motor to a grounded state. There will be no impact on the operation of remaining actuators attached to the same control surface. Once a faulty actuator is identified, the component may easily be replaced, eliminating the need for an expensive and time consuming overhaul or rebuild. Actuator sizing will be determined by the requirements of the flight control surfaces and actuators will be supplied by Parker Hannifin Corporation.

10.4 ELECTRICAL SYSTEM

Electrical power will be provided by two engine mounted 90 kVA Integrated Drive Generators (IDGs) capable of supplying 115/200 V, 400 Hz, three phase AC. The auxiliary power unit houses another 90 kVA generator. Power distribution and management systems as well as power transfer systems will be provided by Hamilton Sundstrand. An auxiliary power unit is necessary to provide a steady supply of electrical power and pneumatic air for engine

start. In the event of an engine failure, the unit will provide pneumatic air and electrical power to aircraft subsystems. As a result, the auxiliary power unit must be certified for continuous operation at all altitudes. An electrically started gas turbine auxiliary power unit will be housed in a firewalled structure in the tail of the aircraft. An inlet duct will be located slightly forward of the vertical stabilizer and exhaust will be ducted through the tailcone. According to Raymer, auxiliary power units have stringent maintenance requirements. Access to the auxiliary power unit will be provided through removable panels located on the underside of the fuselage aft of the main cargo door. Although no particular supplier has been selected at this point, the auxiliary power unit must be certified for continuous operation from sea level to 41,000 ft and must weigh no more than 2,000 lbs.

10.5 Pneumatic System

The aircraft pneumatic system will be supplied with bleed air from the engines, the auxiliary power unit and a pneumatic air cart when on the ground. A cross bleed valve will allow bleed air from either engine to be used to start the opposite engine on the ground or in-flight. The pneumatic system will provide pneumatic air to the OBIGGS system, the cabin pressurization and air conditioning system, the wing, strut and diffuser de-icing system as well as the avionics cooling system.

10.6 Fire Detection & Suppression

An automatic fire detection and suppression system is integral for aircraft survivability and risk mitigation. The system will utilize Firetrace Tubing supplied by Automatic Protection Ltd. This self-activating and self contained system consists of a pressurized extinguishing medium enclosed in a flexible polymer tube placed near potential fire hazards. A flame will melt the polymer tubing to release the extinguishing medium at the flame location. In addition to the

Firetrace Tubing, the automatic fire detection and suppression system will employ ultraviolet-infrared combination sensors to instantaneously detect explosions and control high pressure discharge containers. Smoke and heat detectors will be used to control low pressure discharge containers to suppress fires. This detection and suppression equipment will be supplied by Spectrex Inc.

10.7 SURVIVABILITY

Aircraft survivability will be augmented by a countermeasure dispensing system similar to that currently used on the Boeing C-17 aircraft. The system is manufactured by Symetrics Industries LLC and can automatically detect an anti-aircraft threat, select a dispensable countermeasure, determine a dispersal sequence and release the expendable countermeasure. Countermeasures vary from conventional chaffs and flares to electronic decoys. Missile warning along with infrared search and track functions should be included in this system. The nosecone has space for a 22 in tilt-angle weather, terrain and traffic radar. The supplier for this equipment has not been selected yet.

11 COST ANALYSIS

The RFP states that the flyaway cost and life cycle costs are to be estimated for production runs of 150, 500 and 1500 aircraft. Two methods used to estimate the flyaway cost are outlined in *Airplane Design – Part VIII* by Roskam (Ref. 4) and *Aircraft Design: A Conceptual Approach* by Raymer (Ref. 2). The total life cycle cost was estimated using Roskam's method and was broken down into four sections: research, development, test, and evaluation (RDTE), acquisition, operations, and disposal. All cost estimates are based on the current 2007 US dollar value.

11.1 Research, Development, Test, and Evaluation

The RDTE cost includes all activities that take an aircraft from the planning stage to certification. The RDTE cost includes: airframe engineering and design, development support and testing, flight test airplanes and operations, test and simulation facilities, RDTE profit, and the cost to finance the RDTE phases. The main parameters used to estimate the RDTE cost are TOGW, empty weight, maximum cruise velocity, and the number of static and flight test aircraft produced. The cost estimates are based on four static test aircraft and four flight test aircraft. The RDTE cost will be the same regardless of the number of production aircraft to be produced.

Table 11.1: RDTE Cost Breakdown in Millions of Year 2007 USD

RDTE Cost Category	Cost
Airframe Engineering & Design	$338.3
Development Support & Testing	$99.9
Flight Test Airplanes	$2,001
Flight Test Operations	$15.2
Test and Simulation Facilities	$175.4
Cost to Finance RDTE Phase	$526.1
RDTE Profit	$350.7
Total RDTE Cost	**$3,507**

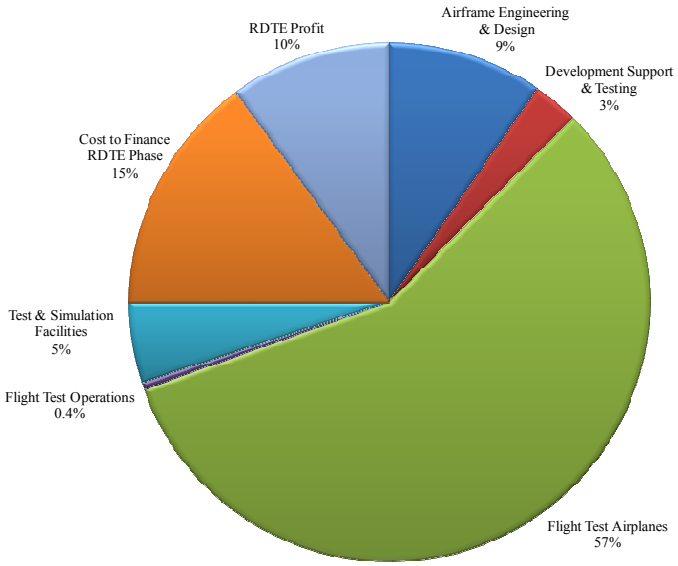

Figure 11.1: RDTE Cost Percentage

11.2 MANUFACTURING AND ACQUISITION

The manufacturing cost is broken down into airframe engineering and design cost, airplane production cost, production flight test operation cost, and the cost to finance the manufacturing phase. The acquisition cost is defined as the manufacturing cost plus the profit made by the manufacturer. A summary of the acquisition cost is shown in Table 11.2.

Table 11.2: Manufacturing and Acquisition Cost Breakdown in Millions of Year 2007 USD

Manufacturing Cost Category	150 Units	500 Units	1500 Units
Airframe Engineering & Design	$246	$385	$544
Airplane Production	$11,400	$30,715	$79,312
Production Flight Test Operations	$62.6	$209	$626
Cost to Finance Manufacturing	$2,066	$5,525	$14,203
Total Manufacturing Cost	**$13,775**	**$36,834**	**$94,685**
Manufacturing Profit	$1,377	$3,683	$9,468
Acquisition Cost	**$15,152**	**$40,517**	**$104,153**

11.3 FLYAWAY

The flyaway cost is an estimate of the unit price per airplane paid by the user of an airplane. The flyaway cost includes the cost of RDTE, manufacturing, and the manufacturer's profit. Table 11.3 below shows the flyaway cost for production runs of 150, 500 and 1500 aircraft. Table 11.4 compares the flyaway cost determined using Raymer's method with the value obtained using Roskam's method. Both methods provide similar estimates and agree to within 2.5% for a production run of 150 units.

Table 11.3: Flyaway Cost Summary in Millions of Year 2007 USD

Cost Category	150 Units	500 Units	1500 Units
RDTE	$3,507	$3,507	$3,507
Manufacturing	$13,775	$36,834	$94,685
Manufacturing Profit	$1,377	$3,683	$9,468
Total Flyaway Cost	**$18,659**	**$44,024**	**$107,660**
Flyaway Cost per Unit	**$124.4**	**$88.0**	**$71.8**

Table 11.4: Comparison of Flyaway Cost in Millions of Year 2007 USD

Production Run	150 Units	500 Units	1500 Units
Flyaway Cost per Unit			
Roskam	$124.4	$88.0	$71.8
Raymer	$127.5	$89.1	$72.7

11.4 OPERATIONS COST

The main contributors to operations cost are the fuel, oil and lubricants, personnel, spares, and depots. Table 11.5 shows the operating costs for the three production runs. The operations cost estimates are based on the following assumptions: a thirty year service life, 1800 annual peace time flight hours, and a fuel price of 2.60 per gallon of year 2007 US dollars.

Table 11.5: Operations Cost Breakdown in Billions of Year 2007 USD

Operations Cost Category	150 Units	500 Units	1500 Units
Fuel, Oil & Lubricants	$32.8	$109	$328
Direct Personnel (Aircrew & Maintenance)	$27.7	$92	$277
Indirect Personnel	$16.5	$55	$165
Consumable Materials (Maintenance)	$2.16	$7.19	$21.6
Spares	$20.3	$68	$203
Depots (Overhaul & Maintenance)	$19.1	$64	$191
Miscellaneous	$8.6	$28.8	$86
Total Operations Cost	**$127.2**	**$423.9**	**$1,272**

11.5 TOTAL LIFE CYCLE COST

The life cycle cost is the cost of the whole program. The cost of disposal is estimated to be 1% of the life cycle cost. Table 11.6 lists the total life cycle cost for the three production runs.

Table 11.6: Life Cycle Cost Breakdown in Billions of Year 2007 USD

Phase	150 Units	500 Units	1500 Units
RDT&E	$3.51	$3.49	$3.49
Acquisition	$15.2	$40.5	$104.2
Operations	$127	$424	$1,272
Disposal	$1.47	$4.73	$13.9
Total Life Cycle Cost	**$147**	**$473**	**$1,393**

12 REFERENCES

1. Keen, Ernest B., *A Conceptual Design Methodology for Predicting the Aerodynamics of Upper Surface Blowing on Airfoils and Wings*. Blacksburg, VA; November, 2004.

2. Raymer, Daniel P. *Aircraft Design: A Conceptual Approach*. 4th ed. Reston: AIAA, 2006.

3. Nicolai. from *Fundamentals of Aircraft Design*. AOE 4065-4066 Design (Aircraft). Mason. *Aircraft Sizing I*. http://www.aoe.vt.edu/~mason/Mason_f/SD1L7.pdf. October 10, 2006.

4. Roskam, Jan. *Airplane Design: Series.* DARCorp. Lawrence, KN; 2005.

5. Kim, Berton, & Jones. *Low Noise Cruise Efficient Short Takeoff and Landing Transport Vehicle Study*. NASA Glenn Research Center, 2006.

6. Marchman, J. *Aircraft Performance Coursepack*. Virginia Tech. Blacksburg, VA; 2003.

7. Byrnes, Hensleigh, Tolve. *Effect of a Horizontal Stabilizer Vertical Location on the Design of Large Transports*. Lockheed, 1966.

8. Farbridge and Smith. *The Transonic Multifoil Augmentor Wing*. NASA Ames Research Center, 1979.

9. *Powered Lift Aerodynamics and Acoustics*. Conference Proceedings.

10. Pratt & Whitney. < http://www.pw.utc.com/StaticFiles/Pratt%20&%20Whitney/News/Image%20Library/Assets/Images/f117_cutaway_high.jpg> 2007.

11. Aerospaceweb.org. *Reducing Landing Distance.* <http://www.aerospaceweb.org/question/propulsion/q0181.shtml> 2007.

12. Pratt & Whitney. <http://www.pw.utc.com/vgn-ext-templating/v/index.jsp?vgnextrefresh=1&vgnextoid=d9e61a157e6db010VgnVCM1000000881000aRCRD> 2007.

13. *Aircraft Design: Synthesis & Analysis.* < http://adg.stanford.edu/aa241/AircraftDesign.html> Desktop Aeronautics, Inc., 2006.

14. Thompson, J.D. *YC-15 Powerplant System Design and Development.* AIAA No. 74-973, 1974.

15. Gundlack, J.F., et al., *Multidisciplinary Design Optimization of a Strut-Braced Wing Transonic Transport*. AIAA 2000-0420 1990

16. LeGresley, Patrick. *Placard Diagram & V-n Diagram*. <http://aero-comlab.stanford.edu/cardinal/design/optimization/vn.m>. 1999.

17. Ko, Andy, et al., *Transonic Aerodynamics of a Wing/Pylon/Strut Juncture*. AIAA 2003-4062 1995

18. Krenkal A.R., Salzman, A., "Takeoff Performance of Jet-Propelled Conventional and Thrust Vectored STOL Aircraft", Journal of Aircraft, Vol. 5, No. 5, 1968.

19. Johnson, William G. *Aerodynamic Characteristics of a Powered, Externally Blown Flap STOL Transport Model with Two Engine Simulator Sizes*. NASA TN D-8057, 1975.

20. Swartz, Karl L. "Great Circle Mapper." 3 March 2007. <http://gc.kls2.com>.

21. J. Kay, W. H. Mason, W. Durham, F. Lutze and A. Benoliel. *Control Authority Issues In Aircraft Conceptual Design: Critical Conditions, Estimation Methodology, Spreadsheet Assessment, Trim and Bibliography.* VPI-Aero-200, 1996.

22. Joel Grasmeyer. *Stability and Control Derivative Estimation and Engine Out Analysis.* VPI-AOE-254, 1998.

23. Murman, E.M., Bailey, F.R., and Johnson, M.L., "TSFOIL — A Computer Code for Two-Dimensional Transonic Calculations, Including Wind-Tunnel Wall Effects and Wave Drag Evaluation," NASA SP-347, March 1975

24. Cotting, Chris, Mike Morrow. *AOE PERF Aircraft Performance Evaluation v.1.3*. VPI-AOE-2006